Master Thesis

International Master of Science in Fire Safety Engineering (IMFSE)

The University of Edinburgh
School of Engineering
Institute for Infrastructure and Environment
Academic Year 2017-2019

Experimental analysis of the relation of porosity of pine needle bulk to the critical heat flux for ignition

Student: Dheeraj Dilip Karyaparambil
Supervisor: Dr Rory Hadden
Submitted on: 30 April 2019

Declaration

"This thesis is submitted in partial fulfilment of the requirements for the degree of *The International Master of Science in Fire Safety Engineering (IMFSE)*. This thesis has never been submitted for any degree or examination to any other University/programme. The author(s) declare(s) that this thesis is original work except where stated. This declaration constitutes an assertion that full and accurate references and citations have been included for all material, directly included and indirectly contributing to the thesis. The author(s) gives (give) permission to make this master thesis available for consultation and to copy parts of this master thesis for personal use. In the case of any other use, the limitations of the copyright have to be respected, in particular with regard to the obligation to state expressly the source when quoting results from this master thesis. The thesis supervisor must be informed when data or results are used."

Total word count: 16565

Main body word count: 14205

30 April 2019

Read and Approved.

Abstract

The impact of porosity of pitch pine needle sample beds on their critical heat flux and time to ignition was experimentally estimated using cone calorimeter in the context of understanding the flammability behaviour of wildland fuel beds. Samples were tested in 63% porous sample baskets and under natural ventilation conditions. The effects of fuel moisture content were not studied in this thesis. Experimental results show that the there is a linear relation between the porosity of the sample beds and the critical heat flux for ignition in the range of 85%-94% porous samples for the species tested. Porosity was found to become less significant with increasing external heat flux as the bulk properties did not make any difference in ignition. It was attempted to separate the effects of convective cooling due to porosity from other dependent variables, such as fuel density and surface-to-volume ratio by carrying out experiments with open and closed baskets. Restricting the airflow through the sample was found to reduce the time to ignition significantly. From post-ignition analysis, it was observed that increasing the external heat flux had little effect on the heat release rate for samples of similar porosity, while the efficiency of combustion and peak heat release rate increased with increasing porosity. Considerable difference in heat release rates with porosity was also observed from post-ignition analysis.

സംഗ്രഹം

വനപ്രദേശത്തെ പൈൻ മരത്തിൻ്റെ സൂചിയില സാമ്പിളിൻ്റെ പോറൊസിറ്റിക്ക് സാമ്പിൾ തീ പിടിക്കുവാൻ വേണ്ടി എടുക്കുന്ന സമയത്തിന്മേലും അതിനു വേണ്ട താപശക്തിയിന്മേലുമുള്ള ആഘാതം കോൺ കലോറിമീറ്റർ ഉപയോഗിച്ചു പരീക്ഷിച്ച് കണ്ടെത്തിയ നിഗമനങ്ങളാണ് ഇതിൽ ഉൾക്കൊള്ളിച്ചിട്ടുള്ളത്. 63% സാമ്പിൾ ബാസ്കറ്റിൽ പ്രകൃതിദത്ത രീതിയിൽ വായു കടത്തിവിട്ടാണ് സാമ്പിൾ ടെസ്റ്റ് ചെയ്തിരിക്കുന്നത്. ഈ പ്രബന്ധത്തിൽ ഇന്ധനത്തിലെ ഈർപ്പത്തിൻ്റെ സ്വാധീനത്തെക്കുറിച്ച് പഠനം നടത്തിയിട്ടില്ല. പോറൊസിറ്റിയും തീ പിടിക്കുവാൻ വേണ്ട താപശക്തിയും തമ്മിൽ ഒരു ലീനിയർ ബന്ധം ഉണ്ടെന്നു പരീക്ഷണങ്ങളിൽ നിന്നു വ്യക്തമായി. എന്നാൽ ഈ ബന്ധം 85-94% പോറൊസിറ്റി ഉള്ള സാമ്പിളുകളിലും ടെസ്റ്റിനു ഉപയോഗിച്ച സ്പീഷിസിലും മാത്രമേ ബാധകം ആവുകയുള്ളു. താപശക്തി കൂട്ടുമ്പോൾ പോറൊസിറ്റിക്ക് ഉള്ള ആ സ്വാധീനം കുറഞ്ഞു വരുന്നു. ക്രിട്ടിക്കൽ താപശക്തിയിൽ വരുന്ന മാറ്റത്തിൽ പോറൊസിറ്റി ആയി ബന്ധം ഉള്ള മറ്റു വേരിയബിളുകളുടെ ആഘാതം വേർതിരിക്കാൻ തുറന്നതും അടഞ്ഞതുമായ സാമ്പിൾ ബാസ്കറ്റ് ഉപയോഗിച്ച് പരീക്ഷണങ്ങൾ നടത്തോകയുണ്ടായി. അടഞ്ഞ ബാസ്കറ്റു കൊണ്ട് വായുസഞ്ചാര നിയന്ത്രണത്തിൽ ഈ സാമ്പിളുകൾ കത്താൻ എടുത്ത സമയം തുറന്ന ബാസ്കറ്റ് സാമ്പിളുകളെക്കാൾ വളരെ കുറവായിരുന്നു. പോറോസിറ്റിയുടെ വർദ്ധനവ് സാമ്പിൾ കത്താനുള്ള കഴിവിനേയും താപ വ്യാപ്തിയെയും അതിന്റെ ഉച്ചസ്ഥായിയിൽ എത്തിക്കുന്നതായി പരീക്ഷണ വിശകലനത്തിൽ കാണുന്നു. പരീക്ഷണ വിശകലനത്തിൽ പോറോസിറ്റിക്ക് താപ വികിരണതോതിലും ഗണ്യമായ സ്വാധീനം ഉള്ളതായി നിരീക്ഷിച്ചു.

Contents

List of Figures

List of Tables

Notations

α	Thermal diffusivity (m^2s^{-1}), Volume Fraction or the inverse of absorption coefficient
α_s	Fraction of solid in the fuel bulk (%)
δ	Radiation penetration depth (mm)
$\Delta H_{c,eff}$	Effective heat of combustion (MJ/kg)
ε	Porosity of the medium (%)
ρ	Particle density (kg/m^3)
ρ^*	Bulk density (kg/m^3)
σ	Surface-to-volume ratio (m^{-1})
ϕ	porosity factor
φ	Porosity (%)
A_s	initial total exposed area of sticks (m^2)
A_v	initial vent area of vertical shafts (m^2)
b	width of each stick (m)
B	Stefan-Boltzmann constant ($5.67x10^{-8}$ $W.m^{-2}.K^{-4}$)
c_p	Heat capacity ($J.kg^{-1}.K^{-1}$)
d	Diameter of the needle (m)
FMC	Fuel Moisture content (%)
FPA	FM global fire propagation apparatus
H	Height of the sample (m)
HRR	Heat release rate (kW)
I_0	External heat flux (kw/m^2)
I(z)	Irradiance at a depth z (kw/m^2)
k	Thermal conductivity ($Wm^{-1}K^{-1}$)

k_R	Rosseland approximation ($W.m^{-1}.K^{-1}$)
K	Radiation attenuation coefficient (m^{-1}) or permeability (m^2)
m_{sample}	Mass of the sample bulk (kg)
MLR	Mass loss rate (g/s)
N	number of layers of sticks
PMMA	Poly(methyl methacrylate)
$\dot{q}''_{cond}$	Conductive heat transferred (kw/m^2)
$\dot{q}''_{i}$	Incident heat flux (kw/m^2)
$\dot{q}''_{crit}$	Critical heat flux for ignition (kw/m^2)
$\dot{q}''_{loss,rad}$	Radiative losses (kw/m^2)
$\dot{q}''_{loss,conv}$	Convective losses (kw/m^2)
$\dot{q}''_{ext}$	External heat flux(kw/m^2)
$\dot{q}''_{min}$	Minimum heat flux for ignition (kw/m^2)
SVR	Surface-to-volume ratio (m^{-1})
t_{chem}	Induction time (s)
t_{ig}	Time to ignition (s)
t_{mix}	Mixing time (s)
t_p	Pyrolyzing time (s)
T	Thickness of the needle (m) or solid phase temperature (K)
T_{ig}	Ignition Temperature (K)
T_∞	Ambient Temperature (K)
V_{sample}	Volume of the sample holder (m^3)
z	Depth inside sample (m)

1. Introduction

Wild fires are a growing threat to human infrastructure and activities both due to climate change and increasing **wildland-urban interface (WUI)**. It has been an important process affecting the Earth's surface and atmosphere for over 350 million years and human societies have coexisted with fire since their emergence. Wildfire, as defined by Oxford Dictionaries (2019), is "a large, destructive fire that spreads quickly over woodland or brush". It is a natural phenomenon that could occur due to natural causes such as climate change, volcanic eruption, lightning, sparks from falling rocks and spontaneous ignition (National Wildfire Coordinating Group., 1998; Scott, 2000). Although it is clear from the study of Doerr and Santin (2016), that USA is among the countries most affected by wildfire, 85% of all wildfires in USA are caused by human activities (U.S. National Park Service, 2019) like arson, damaged power lines, fireworks, camp fires and other accidental fires. Figure 1 shows the change in number of wildfires and the area of forest cover burned down between 1985 and 2017.

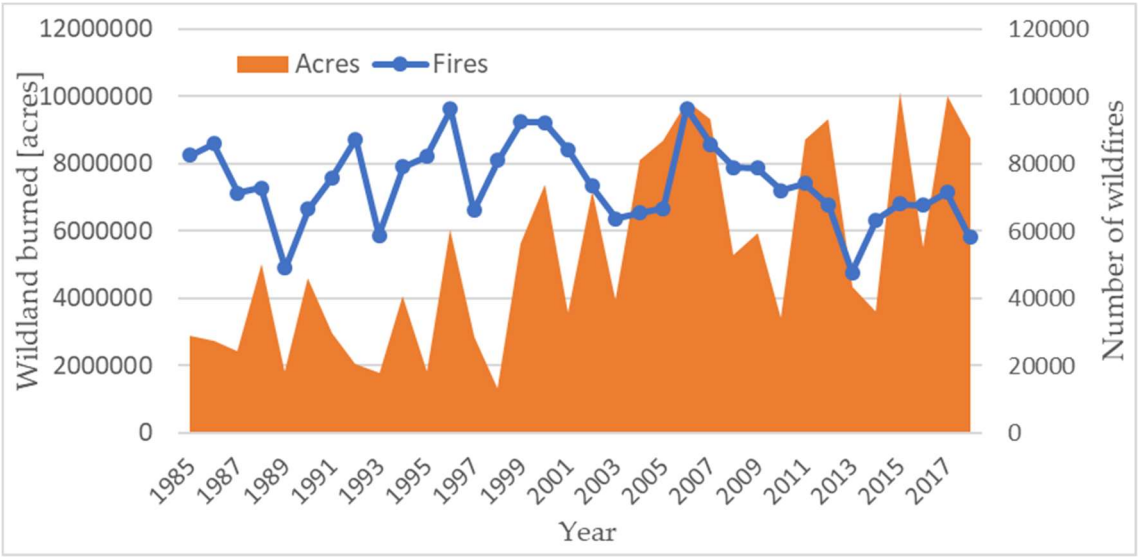

Figure 1: Area burned, number of fires and suppression costs (NIFC, 2017)

The effects of wildfire are quite extensive including environmental, ecological, climatic, economical, health and social ones (C. M. Belcher, 2013). Wildfires destroy sensitive nature,

including endangered plants and animals, and deplete the soil of essential nutrients. Besides, the presence of firefighting water in the soil can cause erosion, the large amounts of smoke released into the atmosphere can cause air pollution, and the ash and smoke can cause serious health problems to exposed personnel. Economic and social effects include the cost of suppression, medical treatments, insurance, reconstruction and rehabilitation, restricted recreational access and loss of livelihood. Figure 2 shows the rise in suppression costs of wildfires between 1985 and 2017. In USA alone, the cost of suppression is well beyond 3 billion USD per year which is evident from analysing Figure 1 and Figure 2. Also, while the number of wildfires per year are going down, the area of forest cover burned down, and the suppression costs are on a rise.

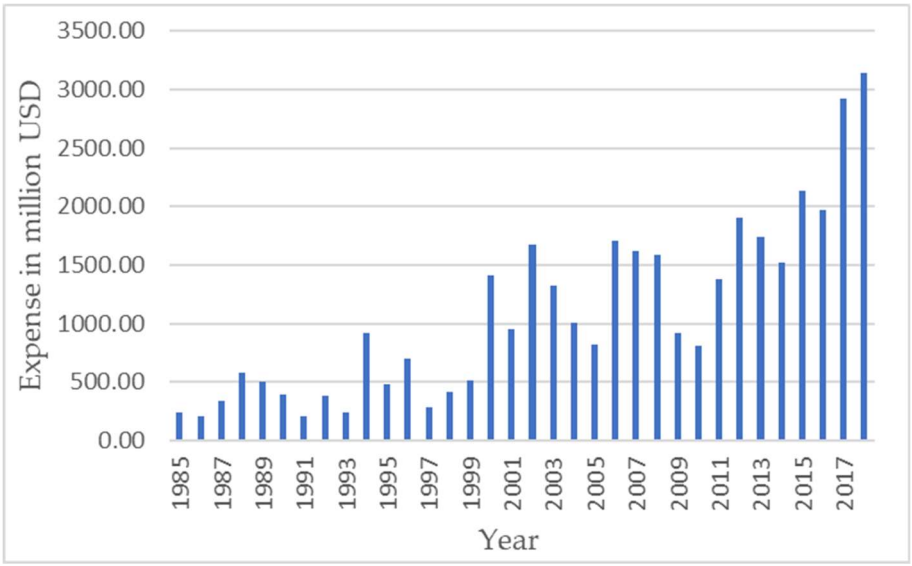

Figure 2: Cost of wildfire suppression with year.(NIFC, 2017)

It is thus critical that the wildland fire professionals need to understand how wildland fuels ignite and burn near WUI. Improved assessment tools are to be developed to help manage the increasing risks and better develop wildland management solutions. The precision of wildland fire assessment tools is limited by the understanding of many key variables (Schemel, 2008). The role of these key variables was found to be more complex from previous experiments. Therefore, research on wildfires becomes essential to understand these key variables.

1.1. Porous Fuel

The forest floor is the most critical element in wild fire spread as the fire usually initiates from there and then spreads vertically through the vegetation or horizontally through the ground. Wildland fuels could be considered as a porous media as it is not one solid particle burning that governs the combustion process, but a volume with several particles influencing each other. This volume will include solid phase (fuel) and a gas phase (normally air), which translates to porosity of the fuel bed (Thomas, 2017).

Porosity of fuel is an important factor while considering flammability and combustion dynamics of a sample as it would drive the oxygen availability to the combustion, determine radiative penetration and cause convective cooling. With more oxygen availability due to natural convection, there could be rapid fire growth and a higher peak HRR, while radiative penetration would determine the rate of pyrolysis, charring and deformation of the fuel bed. Convective cooling becomes important in the sense that it would cool down the fuel and increase the time to ignition for a specific radiative heat flux. In other words, with increased convective cooling, higher radiative heat fluxes are required to ignite the fuel.

However, porosity is not an independent parameter. Thomas, (2017) quotes, "The porosity of wildland fuels introduces a complexity that is ignored for solid material and is explained by bulk properties. This porosity is also highly variable depending on the location of the fuel package (e.g. in the litter layer or in the canopy). Changing the porosity in a fuel package (by varying fuel loading) and keeping other parameters constant will impact the flammability because heat and mass transfer mechanisms are altered". However, changing porosity of a sample would change many other parameters such as density, permeability, fuel load and even the fuel structure at some point.

When the pine needles are just put in a sample holder, they would have a random porosity and some density. As more pine needles are added into the sample holder, the density increases, and porosity decreases. When the density is increased, it means that there is more fuel to undergo

pyrolysis and combust. This would also reduce the permeability of the sample. Santoni *et al.*, (2014) describe permeability as the ability of a fluid to pass through a porous medium. Porosity does not account for the particle sizes and merely defines the fraction of volume of gas to solid. A sample could exist being extremely porous and not at all permeable, for example, closed-cell foam. However, since wildland fuels are not closed-cell, we could say that permeability is related to porosity. The permeability of the fuel can be a function of many variables including degradation and consumption (Torero, 2016) of the material, which are complex processes to study.

Finally, we arrive at a relation where changing one parameter influences many others and it becomes difficult to point out which parameter is responsible for the result that we obtained. This relation could be visualised as,

$$Porosity \propto (Permeability)$$

$$\propto \left(\frac{1}{Density}\right)$$

$$\propto \left(\frac{1}{Fuel\ load}\right)$$

Along with influencing the variables mentioned above, porosity also influences other factors, such as surface-to-volume ratio, radiative penetration, charring depth, re-radiation, and natural convection through the sample.

So how do we conclude that the result obtained is from the effect of porosity, and not from the change in fuel load, permeability, surface characteristics, etc.? Previous studies have found that the role of these parameters is more complex than anticipated and interdependency of multiple parameters to the porosity of the sample makes it a complex variable to study.

1.2. Previous Works

Although all the previously mentioned variables remain important, flow conditions are a key parameter when analysing combustion dynamics of a porous fuel (Bartoli *et al.*, 2011). A porous fuel bed will result in adequate airflow through the sample bulk, consequently enabling more oxygen availability to the combustion than in a non-porous fuel bed where the surface will be the only portion of the fuel on fire with the availability of oxygen being only from the sides.

Schemel *et al.*, (2008) carried out pioneered studies on porosity of sample beds focusing on the effects of transport through porous wildland fuel beds. The tests were done using FPA under natural convection and forced flow with *Pinus halepensis* and *Pinus pinaster*. The test series results were analysed using direct values of measured variables and calculated values of HRR. Heat release rate calculated using calorimetry was compared to mass loss rate and heat of combustion. Discreet variables of time to ignition, duration of flaming and peak HRR were compared using analysis of variance method and it was found that they had strong dependence on fuel species and on flow conditions. The pine needle species studied behaved differently due to different packed densities and different surface-to-volume ratios (SVR). The test series exhibited a high level of repeatability for each test conditions which demonstrated the usefulness of the techniques used in these tests. This test stated that the use of FPA and porous sample holders seemed to increase the reliability of test data.

Schemel, (2008) studied the transport effects through porous wildland fuels using FPA. He did a concept testing with cone calorimeter using 76% and 0% open baskets and tested with a fixed external heat flux of 25kW/m^2. These tests were conducted to see if a new sample holder design could be used in the cone calorimeter and the FPA to determine if the flow effects could be separated and tested using both the devices. However, once this concept was proved, rest of the study was carried out using FPA. The goal of his research study was to conduct an experimental test series, analyse the data and examine the scalability of the results, to determine the effect of transport processes on the HRR of porous wildland fuels.

Bartoli *et al.*, (2011) studied the effects of flow conditions through porous fuel bed (varying basket opening and forced flow conditions) and fuel species on the burning dynamics of pine needles and estimated the time dependent variable HRR, time to ignition, duration of flames and mean HRR. *Pinus pinaster*, *Pinus halepensis* and *Pinus laricio* were the species studied. The sample baskets used were of the size 126 mm diameter and 35 mm depth, with holes on all sides. Baskets with 0%, 26% and 63% openings were used. The results stated that the chemical properties of the fuel species played a prevalent role when the oxygen supply is high enough.

Santoni *et al.*, (2014) assessed the influence of pine needle layer characteristics on combustion for *Pinus halepensis*, *Pinus laricio* and *Pinus Pinaster*. They studied the relationship between permeability of the litter layer, fuel bed porosity and needle geometrical properties, with more focus on the impact of permeability. Their definition of permeability is based on Darcy's Law, and takes porosity and particle size into account and give a reliable relation between porosity and permeability (Thomas, 2017). It was found that the bulk properties did not influence time to ignition for radiant heating of litters in the range of porosities (88-96%) studied and that ignition was mainly driven by SVR. It was stated that a high SVR ensures a rapid ignition of pine needles when exposed to a given radiant heat flux.

Thomas *et al.*, (2014) studied the flammability of different pine needles species under varying air flow conditions using FPA. *Pinus resinosa*, *Pinus rigida* and *Pinus strobus* were the species studied under flow, low flow (50LPM) and high flow (100LPM) conditions. It was found that under natural convection, closed and open baskets gave similar results for time to ignition and twice the peak HRR for open basket than closed basket. They used 15g samples under 25 kW/m2, using 63% porous sample baskets (126 mm diameter, 31 mm depth) to test pitch pine needles.

Finney *et al.*, (2015) described that wildland flame spread is predominantly due to convective heat transfer and had determined that radiation alone is not adequate to allow flame spread in porous wildland fuels. This work is critical since many of the existing models consider radiation heat transfer as the main mechanism of fire spread. Their work shows how complex the fire

spread mechanism really is and how much of the physical mechanism is misinterpreted or still unknown. This brings more importance in studying the heat transfer mechanisms involved in a porous media where convective and radiative heat transfer would create complex heat transfer scenarios before ignition.

Thomas (2017) stated that the pine needles remained to be thermally thin till 60kW/m^2 and found that increasing the flow of oxygen through the sample has no effect on the ignition. In this experiment, a similar test was done with open (flow) and closed (no airflow) basket conditions and the mass loss rate before ignition (pyrolysis rate) was compared to his results. Thomas (2017) did experiments with *Pinus strobus, Pinus resinosa* and *Pinus rigida*. He found that surface-to-volume ratio was one of the key driving factors behind faster ignition for *Pinus strobus* needles and concluded that fuel moisture content was a single variable to predict ignition.

Ravena, (2019) had done very similar tests to this study to determine the relation of porosity on time to ignition. He used FPA as well, but the samples were tested under closed basket (no flow) conditions (baskets covered in aluminium foil). He tested for 97%, 94%, 90%, 85%, 75%, 62% and 51% porosities under 25 kW/m^2 and found that least time to ignition was around 85% porosity but that the ignition times tend to increase when increasing or decreasing porosity.

Table 1 lists some of the previous studies on pine needle flammability and it should be noted that almost all the studies were done using FPA and none of them tried to relate porosity of the bulk bed with critical heat flux (CHF).

Table 1 - FPA experimental conditions from literature (Ravena, 2019)

Date	Author	Ref.	Pinus	Mass	Sample Holder	Conditions	Heat Flux
2008	Schemel	(Schemel *et al.*, 2008)	Halepensis (unconditioned)	15g	0%, 26%, 63%.	Air 0L/min, 200L/min.	25kW/m^2
		(Schemel, 2008)	Pinaster (unconditioned)	15g	0%, 26%, 63%.	Air 0L/min, 200L/min.	25kW/m^2
2011	Bartoli	(Bartoli, 2011) (Simeoni, 2011)	Halepensis (unconditioned)	10g, 12g, 15g, 20g.	0%, 26%, 63%.	Air 0, 100, 200L/min.	25 kW/m^2
			Pinaster (unconditioned)	11g, 13g, 15g, 17g.	0%, 26%, 63%.	Air 0, 100, 200L/min.	25,30,35,40 kW/m^2
			Laricio (unconditioned)	10g, 13g, 15g, 20g.	0%, 26%, 63%.	Air 0, 100, 200L/min.	25 kW/m^2
2011	Bartoli	(Bartoli *et al.*, 2011)	Halepensis (unconditioned)	4g, 15g.	0%, 26%, 63%.	N2 60L/min; Air 0, 100, 200L/min.	25 kW/m^2
			Pinaster (unconditioned)	4g, 15g.	0%, 26%, 63%.	N2 60L/min; Air 0, 100, 200L/min.	25 kW/m^2
			Laricio (unconditioned)	4g, 15g.	0%, 26%, 63%.	N2 60L/min; Air 0, 100, 200L/min.	25 kW/m^2
2011	Mindykowski	(Mindykowski *et al.*, 2011)	Pinaster	5g, 10g, 20g.		Air 0L/min.	30 kW/m^2
		(Jervis Calle, 2012)	Halepensis (live,aged, dead)	8g	0%; 63%	Air 0L/min; 200L/min.	50 kW/m^2

2012	Jervis	(Jervis and Rein, 2016)	Halepensis	3g, 5g, 8g, 10g, 12g, 15g, 20g.	63%	Air 0L/min; 200L/min.	25; 35; 50 kW/m^2
			Nigra	3g, 5g, 8g, 10g, 12g, 15g, 20g.	63%	Air 0L/min; 200L/min.	25; 35; 50 kW/m^2
			Pinaster	3g, 5g, 8g, 10g, 12g, 15g, 20g.	63%	Air 0L/min; 200L/min.	25; 35; 50 kW/m^2
2016	Thomas	(El Houssami *et al.*, 2016; Thomas, 2017; Thomas, Hadden and Simeoni, 2017)	Strobus	15g	0%; 63%	14-23%O2 Air 0;50;100;200L/min	10-60 kW/m^2
			Resinosa	15g	0%; 63%	14-23%o2 Air 0;50;100;200L/min	10-60 kW/m^2
			Rigida	15g	0%; 63%	0L/min	25; 50 kW/m^2
2018	Ravena	(Ravena, 2019)	Rigida	7.5g 15g 25g 35g 60g 95g 120g	0%	0L/min	25 kW/m^2

1.3. Wood cribs

Wood cribs are among the most widely studied organic sample in fire science. Can results from wood crib studies be extrapolated to fit the results from pine needle studies? According to McAllister and Finney, (2016) stated the burning rate increases with the inter-stick spacing or the ''porosity'' of the crib if the cribs are in the densely-packed regime. This concept resembles the one of porosity adapted for pine needles in this study, which is that the porosity is higher when there is more space between the needles. Besides that, the burning rate increases with porosity factor, as far as it is in the densely-packed regime. Beyond that regime, there will not be enough fuel to cause sustained burning and the burning rate would not be affected.

The porosity of wood cribs is calculated as porosity factors using the equation (Gross, 1962),

$$\phi = N^{0.5} b^{1.1} \frac{A_v}{A_s} \qquad (1.1)$$

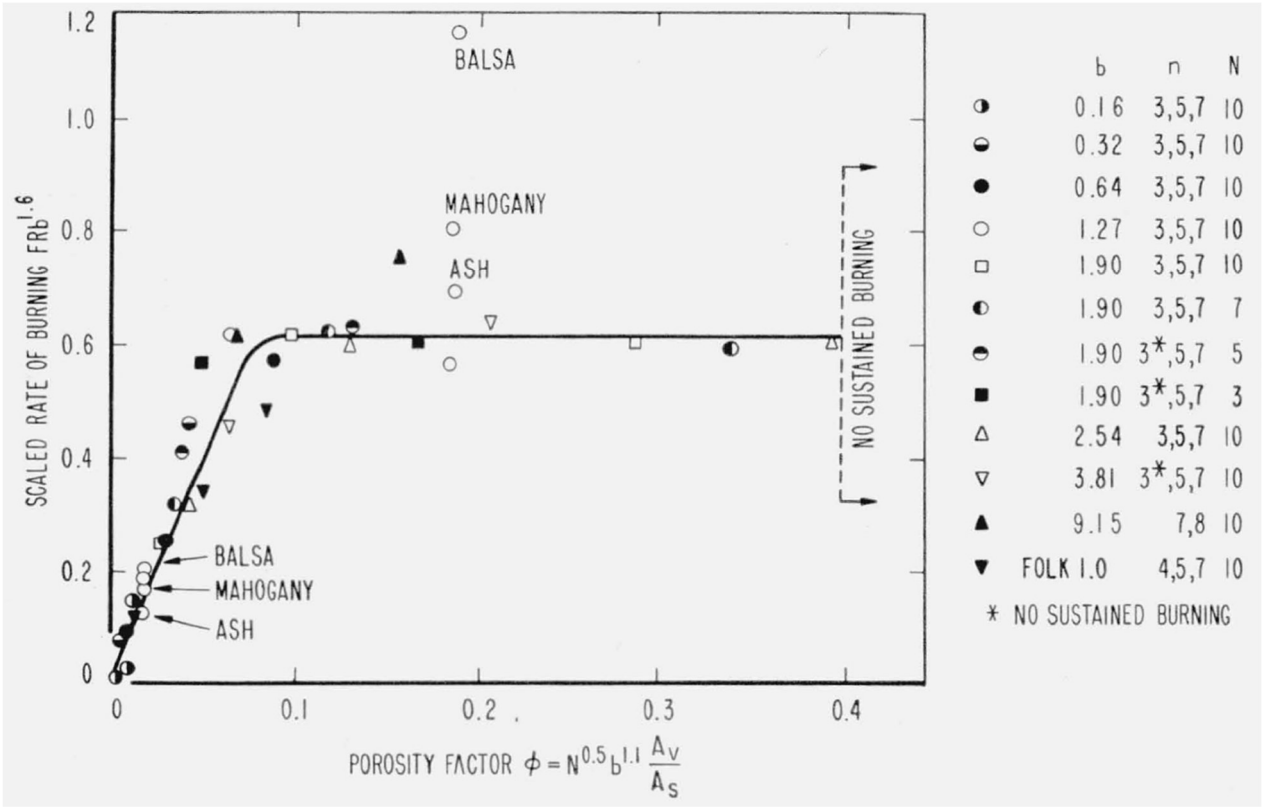

Figure 3: Effect of porosity on the scaled rate of burning (Gross, 1962).

Where ϕ is the Porosity factor, N is the number of layers of sticks, b is width of each stick, A_v is the initial vent area of vertical shafts and A_s is the initial total exposed area of sticks.

If we calculate the porosity factor for pine needles 1.39 mm wide packed in bulk at 94% porosity with approximately 15 layers and 20 needles per layer, we obtain ϕ=0.03. Although the porosity factor is calculated differently from the way porosity is calculated for pine needle samples in this study, they do have some relation based on the availability of voids in the fuel bulk. According to Figure 3, until ϕ=0.1, there is a rapid change in rate of burning with porosity factor. We could relate this to pine needle terms and say that until the number of pine needle in the bulk is very low (one or two needles) that they start acting as individual needles, there will be a considerable change in burning rate with change in porosity.

1.4. Problem Definition

Fires occurring in nature are extremely complex to study in a single attempt. They could be approached in micro (studying the individual fuel characteristics contributing to wild fire) or macro scales (studying the behaviour of the fire itself). If we study the fundamentals at micro scales, it would be easier to extend that knowledge into predicting the behaviour of wild fires in all scales. However, along with the extend of spread of the fires and the external parameters that may influence the fire, the nature and structure of the fuel itself could make it complex to study in a micro scale. The vegetative fuels may vary widely in size and structure of the fuel bulk.

Fuel flammability is also an integral part of understanding wildfire behaviour as it helps to understand the ignition and combustion dynamics. These flammability characteristics could then be extrapolated using wildland fire models to model fire at macro scales.

This study, along with many others in the past, will try to address the wild fire problem at a micro scale, focusing on porosity of the fuel bulk which is one of the many fuel parameters influencing the flammability characteristics of fire. Critical heat flux being one of the most crucial

flammability characteristics had never been related with the porosity of the fuel bed in any of the previous studies, which along with the fact that most experiments were done in FPA and not cone calorimeter, are the motivations to conduct the experiments presented in this thesis.

1.5. Objectives

The primary objective of this thesis is to estimate the relation of critical heat flux for ignition with porosity of the wildland fuel sample. It will also be attempted to plot a graph showing the variation of external heat flux with inverse square root of time to ignition.

If adequate experimental results will be available, it will be attempted to estimate the influence of porosity on other parameters such as time to ignition, pyrolysis rate and heat release rate. In addition, the dependence of external heat flux on heat release rates and time to ignition will also be analysed. The influence of air flow and no air flow on a sample is also expected to be studied.

2. Theory

2.1. Wildland fuel sample – *Pinus rigida*

Pitch pine (*Pinus rigida*), one of the most common pine species in North-Eastern USA and parts of Canada, was studied in this thesis. They are among the most flammable fuels in a forest and is present throughout the year. Some properties of pitch pine needles are given in Table 2 and Figure 4 shows the basic test setup followed with dimensions of the sample basket.

Table 2: Pitch Pine properties

Property	Value
Particle Density (ρ)	607.5 kg/m^3 (Thomas, 2017)
Surface-to-volume ratio (SVR)	4776 m^{-1} (Thomas, 2017)
Diameter of one needle (d_{needle})	1.39 mm (Thomas, 2017)
Heat capacity (c_p)	2069.7 (J.kg^{-1}.K^{-1}) (Thomas, 2017)
Thermal conductivity (k)	0.112 (Wm^{-1}K^{-1})(Tihay *et al.*, 2009)
Thermal inertia (k ρ c_p)	1.41 x 10^5 (W^2.s.m^{-4}K^{-2}) (estimated)
Thermal diffusivity (α)	8.9 x 10^{-8} (m^{2}s^{-1}) (estimated)
Thickness (mm)	0.5 (mm) (assumed as per Simeoni *et al.*, (2012))

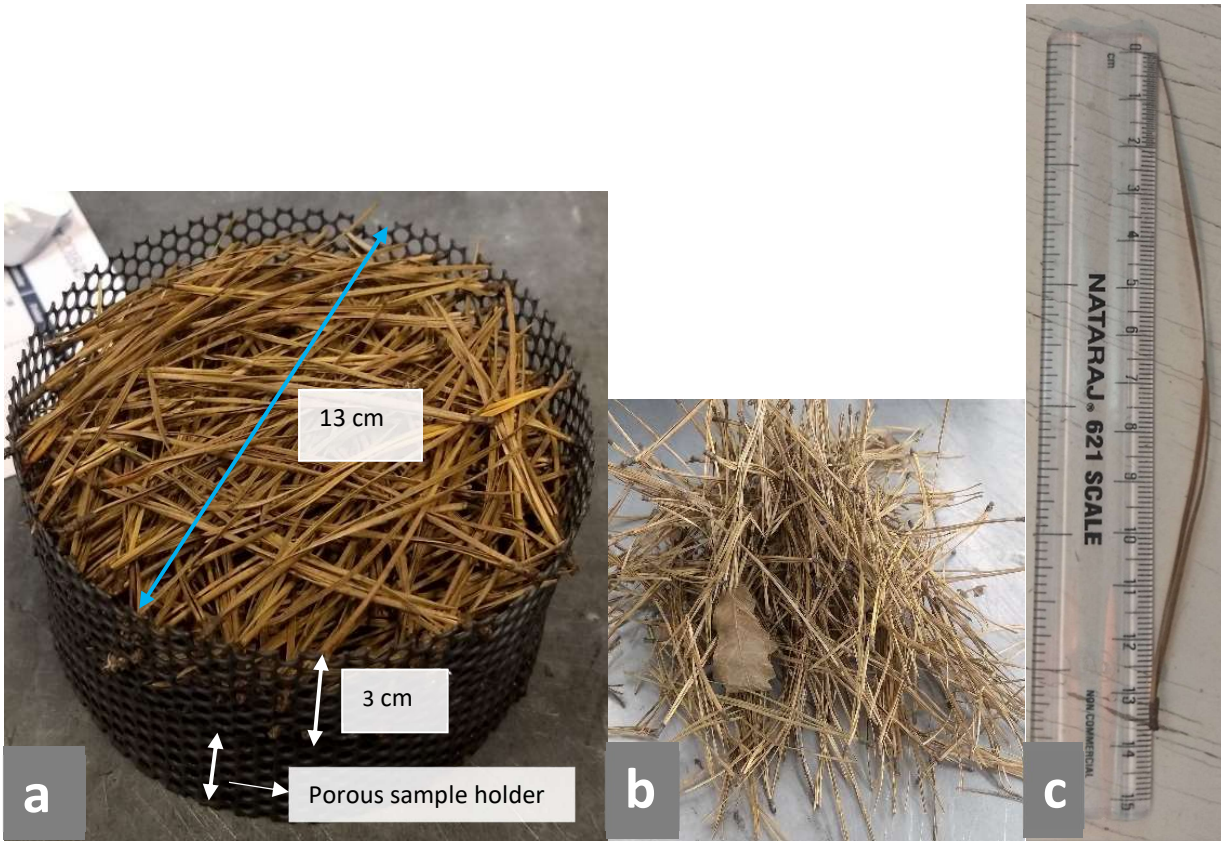

Figure 4: a) Sample basket dimensions b) Pine needles before packing. C) One pine needle against a 15 cm long ruler.

The particle density (ρ) is the effective density of a single pine needle and not the entire sample bulk. A pine needle has a hard, fibrous outer shell, a delicate interior, and a fibrous central core. The outer protective layer, or epidermis, is composed of elongated cells with thick external coating of waterproof material (Howard, 1973). However, it also has an inherent porosity. The density mentioned in Table 2 is the density of dead needles.

2.1.1. Bulk Density and Porosity

The bulk density of the fuel sample, as stated in Thomas *et al.*, (2014), is calculated from the sample weight and the volume of sample holder using the equation

$$\rho^* = \frac{m_{sample}}{V_{sample}} \qquad \textit{(Equation 2.1)}$$

where, ρ^* is the bulk density (kg/m^3), m_{sample} is the mass of the sample bulk (kg) and V_{sample} is the volume of the sample holder.

The bulk density and particle density (ρ) was used to calculate the porosity (φ) of the sample using the equation

$$\varphi = 1 - \frac{\rho^*}{\rho} \qquad \textit{(Equation 2.2)}$$

When φ=0, we could say that the fuel is not porous at all as particle density is same as the sample density.

2.1. Heat transfer through porous media

Heat transfer within and around the fuel is important to understand the behaviour of samples under various conditions. There are three basic mechanisms of heat transfer, namely conduction, convection and radiation. Conduction is the energy transfer from one body to the other by direct contact. Convection is the energy transfer through motion of medium between two bodies. Radiation is the energy transfer from one object to the other through electromagnetic waves. While most of the fires would have all the three methods of heat transfer, one of them may predominate the other at different stages of fire (Drysdale, 2011).

When exposed to a heat source, surface temperature of a solid increases due to the heat transferred to it and this heat is then transferred into the bulk through conduction. In a similar process, heat is lost at the surface too. If heat from the surface of the material is transferred to an external object via conduction, convection or radiation, then, at some point, the surface of the

object will be at lower temperature than its interior bulk. In such a case, there will be energy transfer from the bulk of the object to its surface as per the second law of thermodynamics. A flow through the surface of the object by a fluid at lower temperature (or energy) than the surface would take away heat from the surface of the object and if the fluid is at a higher temperature, it would transfer energy to the surface of the object under normal conditions. There could also be heat losses due to re-radiation from the surface of the exposed body (Thomas, 2017).

In porous samples, due to relatively larger distances between adjacent particles from the presence of voids or air gaps, conduction in the fuel matrix could be ignored and it could be said that heat transfer occurs mainly due to radiation and convection (Thomas, 2017). However, there could still be conduction within the individual particle, which would lead to pyrolysis, as explained in the following section.

The heating condition of a given volume of fuel could change over time during a realistic wild fire scenario. Initially, the fuel package far from the fire front would be in thermal equilibrium with ambient conditions. As the fire grows closer, the particles in the fuel package will experience radiant heating from the flames and convective cooling due to the airflow through the fuel bulk, simultaneously. As the flame front moves closer to the fuel bulk, the intensity of radiative heating increases. At some point, the heat transferred by radiative heating will be more than the heat lost due to convective cooling. Moreover, the ambient temperature itself could increase with approaching fire front and the temperature of the air flowing through the sample would increase and convective cooling would gradually become convective heating. Eventually the fuel particles will be engulfed in flames bringing radiative and convective heating to their maximum (Thomas, 2017).

This transient heat transfer problem is quite complex. There will be uncertainties in analysis if steady state conditions are assumed or if we ignore certain heat transfer mechanisms. A condition with only convective heat transfer would not exist as there will always be heat being radiated from the flames. Radiative heating cannot exist independently as well since there will

be movement of air through the sample causing convective heating or cooling. A combination of both convective and radiative heat transfer would be the only solution which may also help to identify the extent of simplification possible with an acceptable error (Thomas, 2017).

2.1.1. Pre-ignition stage

Although some post-ignition characteristics were analysed, only pre-ignition condition was studied in-depth, since once the sample was ignited, its structure changed, and it was quite complex to analyse the processes going on.

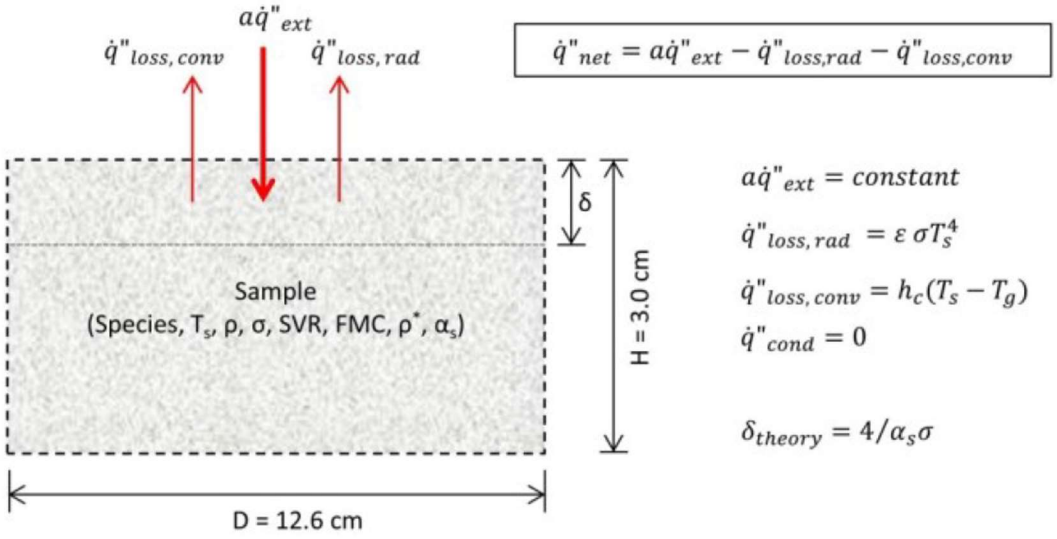

Figure 5: "Sample schematic with simplified heat transfer balance (stage 1)"

(Extracted from Thomas, (2017))

Thomas, (2017) had produced a clear schematic of heat transfer scenario for porous fuel beds as shown in Figure 5. At pre-ignition stage, external heat flux ($\dot{q}''_{ext}$) is the radiant heat flux applied from the conical heater of the cone calorimeter. Heat losses would occur at the solid-air interface at this stage and it could be due to convective cooling from the airflow (natural convection) through the sample, convective heat transfer to the air at the exposed surface of the sample which when gets heated, is being replaced by colder air from the surroundings, and due to re-radiation from the sample itself.

The external radiation can penetrate the sample to a maximum depth defined as the radiative penetration depth (δ)(Wickström, 2016). It means that the particles are also heated up within a volume beneath the surface and not just on the surface of the sample. Radiation intensity, type of radiation source, properties of the fuel particles and bulk properties of the fuel bed are the parameters that could determine the depth of radiation penetration (Thomas, 2017).

Since only natural convection is tested for in this study, although the convective coefficient h_c will be dependent on the flow magnitude, it will remain in the range of 5-25 W/m^2.K (Drysdale, 2011). The porosity and permeability of the fuel bed would decide the actual flow of air through the fuel bed and thus vary the heat transfer coefficient.

Santoni *et al.*, (2014) gave a correlation for porosity and permeability with the equation

$$K = \frac{\varepsilon^3}{20(d/T)^4\,(1-\varepsilon)^2\sigma_P^2} \qquad \textit{(Equation 2.3)}$$

Where K is the permeability (m^2), ε is the porosity of the medium, d is the diameter of the needle (m), T is the thickness of the needle (m) and σ_P is the SVR (m^{-1}). If we calculate the permeability for our *Pinus rigida* samples, assuming a similar value as taken for *Pinus halepensis* in Santoni *et al.*, (2014) which is T~0.5mm, they will result in the values as shown in Table 3. However, it should be noted that 85% porosity was out of the range of application stated for the equation which was 88%-96%. It is still possible to understand that a trend of reducing permeability exists with reduction of porosity.

Table 3: Permeability of samples

Porosity	**Permeability, K (10^{-9} m^2)**
94%	8.46
90%	2.6
85%	1

2.1.1.1. Radiative heat transfer

Lack of a well-defined surface area and the porous structure of the fuel bulk causes the radiative heat to be transmitted to some depth into the bulk. The energy transmitted by the radiation gets attenuated at this depth and it results in particles of the fuel getting heated up. Grishin *et al.*, (2002) found that the radiation attenuation in pine needle beds follow Beer-lambert law, which was applied in Simeoni *et al.*, (2012) to estimate the radiative penetration depth for *Pinus halepensis* needle beds. Where $I(z)$ is the irradiance at a depth z from the surface, I_0 is the external heat flux, and K is the radiation attenuation coefficient ($K = 1/\delta$), the equation (Vaz, André and Viegas, 2004; Thomas, 2017) is as follows

$$I(z) = I_0 e^{-K} \qquad \textit{(Equation 2.4)}$$

Even though it underestimates the value, De Mestre *et al.*, (1989) had come up with a more simplified correlation for estimation of radiative penetration depth as the inverse of absorption coefficient α, as given below.

$$\alpha = \frac{s_f Q_b}{4 Q_f}$$

Where s_f = Surface to volume ratio (SVR) (m^{-1}), Q_b = Density of the fuel sample bulk ($kg.m^{-1}$), Q_f = Density of the fuel ($kg.m^{-1}$), Q_b/Q_f could be expressed as α_s and $1/\alpha$ as δ. The equation could be rewritten as,

$$\delta = \frac{4}{\alpha_s \sigma} \qquad \textit{(Equation 2.5)}$$

α_s is the fraction of solid in the fuel bulk, whereas porosity is $1 - \alpha_s$ as shown in $\varphi = 1 - \frac{\rho^*}{\rho}$ (Equation 2.2). This shows that radiant heat transfer in a porous media has strong dependency to porosity of the fuel bed. Vaz, André and Viegas (2004) found that radiation attenuation gets stronger as the fuel beds get denser, which means that the radiative heat transfer occurs in a larger volume beneath the surface of the fuel bed as the

porosity of the bed increases. While in a denser fuel bed with lower porosity, the volume of fuel the heat gets transferred to is lower. This means the heat transferred to each particle in the volume being exposed to is higher than that for the high porosity case. In other words, the temperature gradient through the depth of the fuel bed depends on the porosity (Thomas, 2017).

Temperature gradient in a solid material is determined by thermal diffusivity ($\alpha = k/\rho c_p$), where k is the thermal conductivity, ρ is the density and c_p is the heat capacity. As stated in Torero, (2016), a heat wave propagates faster through a material with higher values of α. Which means that the surface of the material heats up slower. In the case of porous fuel bed, since the conductivity of the bulk is considered negligible, a new parameter had to be introduced to describe in-depth radiation heat transfer.

Simeoni *et al.*, (2012) neglected the absorption of radiation in the gas phase due to the presence of pyrolysis gases and devised a model which takes the in-depth radiation into account to represent the impact of external heat flux through the porous matrix. Later, they linearized the radiative heat transfer using the Rosseland approximation and introduced the parameter k_R, which replaces the conduction heat transfer term in general heat balance and is expressed as:

$$k_R = \frac{16}{3K} BT^3 \qquad \textit{(Equation 2.6)}$$

Where, B is the Stefan-Boltzmann constant (5.67×10^{-8} W.m^{-2}.K^{-4}), K is the radiation attenuation coefficient as in $Iz = I_0 e^{-Kz}$ (Equation 2.4)) and T is the solid phase temperature. If for simplification T is considered constant, when porosity of the fuel bed increases, the K is reduced which increases the k_R. This would mean that the radiation energy is transferred more easily through the fuel bulk. This could be compared with the thermal conductivity of a material where increasing the conductivity would result in better energy transfer through the material. When energy is transferred better, it results in the surface temperature increasing slower, as the heat is being transferred from the surface into the bulk

more efficiently. If the thermal conductivity is low, the sample surface would get heated up faster as less heat is being transferred to the bulk of the sample (Thomas, 2017).

The application of this equation could not be carried out on the experiments done since the solid phase temperature is not available. Maybe it could be done in future studies where adequate data is available.

Thomas, (2017) states that the denser the fuel bed is, the more energy it stores and faster it pyrolyzes compared to fuel beds that are less dense. In other words, a fuel bed with higher porosity (or less dense) would take longer time to pyrolyze. However, this is just by considering radiant heating and not taking convective cooling into account.

2.1.1.2. Convective heat transfer

Only natural convective flow and no forced flow is tested for in this study. In a realistic wildfire scenario, only natural convection would exist. Although fire fronts could cause an elevated convective air flow through porous fuel bed, this study does not take such strong flows into account.

Convection could either cause cooling or heating depending on the temperature difference between the body and the fluid (air in this case). It could either cause cooling, wrestling against the radiative heating or it may contribute further to heating through hot gases or flames itself. In our case, convection is mainly due to the natural convective motion of air inside the fuel bulk. This mechanism depends on the size of particles, since the heat transfer increase with increasing SVR, and porosity, since it decides the flow of air through the sample (Thomas, 2017).

As the SVR of the fuel bulk increases, convective cooling also increases as a larger surface area is available for cooling. However, this also means that more radiation is absorbed due to larger surface area. While radiant heating occurs at the surface, convective cooling could take place throughout the perimeter of the fuel particle. As a result, convective cooling may dominate and the net heat transfer to the solid fuel particles may be reduced. This means that much higher

radiant heat fluxes are required to ignite a small particle compared to a larger particle under the same ambient conditions. The airflow through the fuel bulk in a simplified form using cylindrical particles is shown in Figure 6.

Flow through the sample occurs from the sides and the bottom of the sample when the air above the exposed surface of the sample basket gets heated and moves up. When this air moves up, it creates a pressure drop and make colder air move in to replace it. While majority of the air that replaces the hot air layer would move in directly from outside the sample basket, some of the air would move in through the sample from the bottom and sides of the basket. This could be explained as buoyant air creating a suction effect on the surface of the sample.

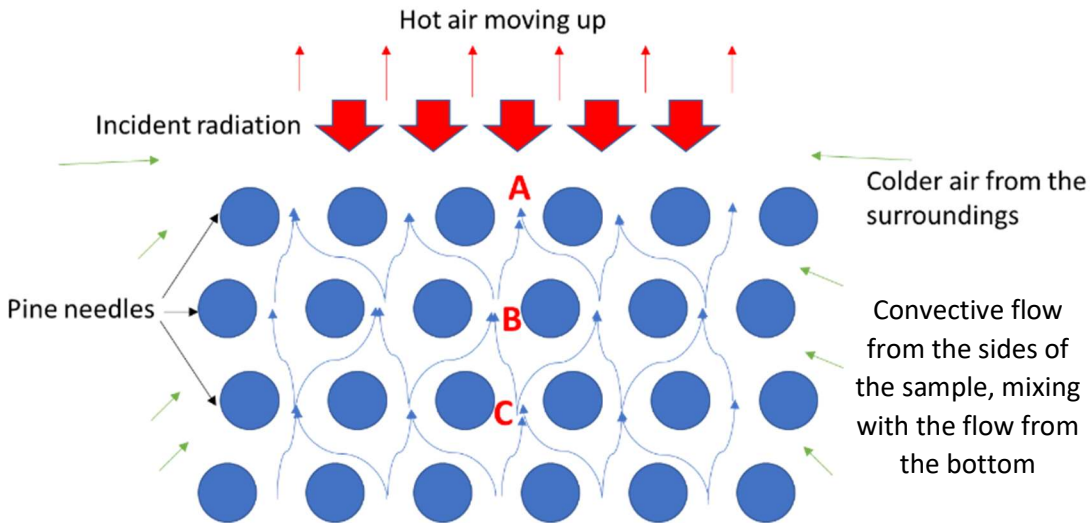

Figure 6: Simplified visualisation of air movement through the sample.

This convective motion of air could also be simplified as colder air from a void beneath the surface of the sample, moving up to replace air which had moved up due to buoyant forces when it was heated. Figure 6 shows the movement of air through the sample in a simplified diagram. When air from void A is heated and moves up, the air from void B replaces it while air from void C replaces the air in B.

Since the flow is due to buoyant flow created by air heated up at the surface of the fuel bed by the external heating source, and since flow happens from all sides simultaneously mixing with

each other, it is challenging to apply any conventional correlations, as given by Rohsenow and Hartnett (1998), Bejan and Kraus (2003) or A. Nield and Bejan (2006), to predict or model the flow with any useful levels of accuracy.

2.2. Ignition of solids

When a solid material at ambient temperature (T_0), is introduced to an external heat source, the temperature of the surface exposed to the source increases. The onset of ignition process will be defined as this moment at t=0. A series of physical and chemical phenomena are initiated at the surface of the material at this moment (Torero, 2016).

The energy received at the surface of the solid is conducted through the depth of the solid, to the unexposed sides, governed by the thermophysical properties of the material. The energy transfer through the depth of the solid creates a thermal gradient varying with depth and with time. When the heat transfer through the solid from the exposed surface is not efficient enough, the surface attains enough temperature to pyrolyze (Torero, 2016).

Pyrolysis tends to be an endothermic process controlled by many chemical reactions which are strong functions of the temperature (Torero, 2016). These pyrolysis gases or fuel vapours emerge through the exposed surface and mix with air in the boundary layer. Under certain conditions, this mixture exceeds the lower flammability limit and ignites when they encounter a source of ignition (Janssens, 1991). The time to ignition could be expressed as the sum of pyrolyzing time (t_p), mixing time (t_{mix}) and induction time (t_{chem}) as given below:

$$t_{ig} = t_p + t_{mix} + t_{chem} \approx t_p$$

Pyrolyzing time is the time required for the fuel to heat up to achieve pyrolyzing temperature (T_P). Mixing time is the time required to form an air-fuel mixture of pyrolysis gases and oxidizer above the material. Induction time is the time required for the flammable mixture to reach its critical temperature at which a chemical runaway or combustion occurs (Drysdale, 2011).

Since the mixing time and induction time are relatively much lower than pyrolysis time for solid fuels under natural flow conditions, they are usually overlooked. However, in the case of porous, open-celled fuels, there could be convective cooling and dilution of flammable mixture due to forced flow through the fuel bed, which would result in delayed ignition. Convective cooling of the porous fuel bed could cause the surface temperatures of the fuel to lower and result in lowering the rate of pyrolysis. It could also be argued that air-fuel mixture could be formed faster due to better mixing. The exact behaviour is difficult to predict and would depend on the balance between the pyrolysis gases and oxidizer flow (Thomas, 2017). Similar effects may be expected from natural flow conditions with much less intensity in case of porous fuels as there is still a flow through the fuel bed although not forced. These effects may cause variations in the pyrolyzing, mixing and induction times.

The three modes ignition could occur are 1) piloted ignition when the pyrolysis gases are ignited at the pilot flame; 2) auto/spontaneous ignition in the absence of a pilot flame; 3) smouldering to flaming where the gases are ignited due to the presence of smouldering. Piloted ignition is most studied due to most repeatable conditions ideal for flammability tests and it will be used in this study as well (Babrauskas, 2003; Thomas, 2017).

Flaming combustion initiated in the vicinity of a small pilot located in the boundary layer is called piloted ignition (Janssens, 1991). The pilot is an electric spark for cone calorimeter (Babrauskas, 2016) which is the apparatus used for this study. Summarizing the ignition process of the sample, it requires the heating up of the sample surface to a pyrolyzing temperature by an external heat source, production of pyrolysis gases exceeding the lower flammability limit of the fuel, mixing of pyrolysis gases with air, transport of this mixed gas to the pilot, ignition of the gas mixture by the pilot. In the presence of a pilot, it could be assumed that ignition occurs when a flammable mixture is present at the location of the pilot (Torero, 2016).

Heat flux

External heat flux could be produced by a convective, conductive or radiative source. Janssens, (1991) defined the minimum heat flux level below which ignition under practical conditions cannot occur as minimum heat flux for ignition ($\dot{q}''_{min}$). He also defined critical heat flux for ignition ($\dot{q}''_{crit}$) as an estimate derived from a correlation of experimental data which is defined as the irradiance resulting in ignition criterion being fulfilled at time $t_{ig} \rightarrow \infty$. It is usually lower than $\dot{q}''_{min}$ and therefore a conservative estimate of the minimum heat flux for ignition (Janssens, 1991). Since $\dot{q}''_{crit}$ is obtained by extrapolating to $t_{ig} \rightarrow \infty$, this may be done by plotting $\dot{q}''_{crit}$ vs t_{ig} and extrapolating the asymptotic value of $\dot{q}''_{crit}$ (Drysdale, 2011) as shown in Figure 7.

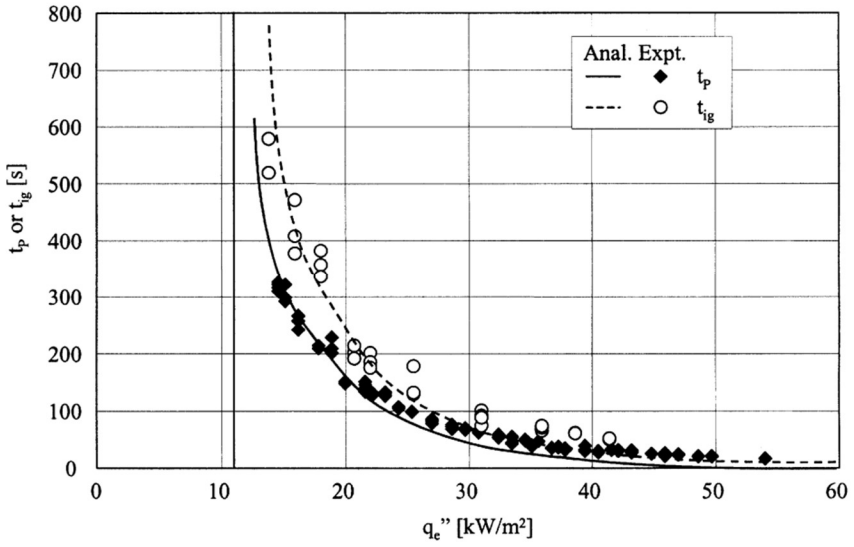

Figure 7: Characteristic ignition delay times (tig) and times to the onset of pyrolysis (tp) for PMMA and a wide range of external heat fluxes. (Dakka, Jackson and Torero, 2002)

Janssens (1991) states that $\dot{q}''_{crit}$ depends on the model to correlate the data since it is the result of an extrapolation and that it should be treated with caution. He advices to treat this as a theoretical value and that it should just be one of the fitting parameters in the correlation.

In this thesis, the $\dot{q}''_{min}$ will be considered as $\dot{q}''_{crit}$ due to the statement above and since there are quite a lot of uncertainties and complexities that exist while trying to study the flammability characteristics of porous wildland fuels as stated in previous sections.

3. Experiment

As explained in the previous chapters, the objective of this study was to experimentally determine the relationship of porosity of fuel bed and the critical heat flux for ignition, which would help to understand the effects of forest floor densities (or porosities) on their ignition characteristics.

FM Global Fire Propagation apparatus (FPA) was used in most previously carried out studies on pine needle flammability as they were trying to control the ventilation properties. However, since in this experiment, only natural ventilation is considered and due to other considerations mentioned in the next sections, it was decided to use cone calorimeter.

3.1. Apparatus

Why Cone Calorimeter and not FPA

From Schemel *et al.*, (2008), Simeoni *et al.*, (2012), Santoni *et al.*, (2014) and Bartoli *et al.*, (2015), it is evident that almost all the flammability tests for pine needles were carried out using Fire Propagation Apparatus and not cone calorimeter. This could be related to the expected results of these tests, where most of them were trying to find the relationship of different parameters to the airflow. Unlike in Cone Calorimeter, FPA can analyse fire behaviour in specific ventilation conditions by altering the inflow air characteristics. FPA considers the flames from the burning material to characterize fire and increases accuracy of HRR calculations by considering CO_2 and CO (ASTM E-2058, 2003).

While cone calorimeter uses a conical electrical heater to produce heat flux, the same is achieved by infrared tungsten lamps in FPA. This difference in heating element would also affect the way the needles undergo pyrolysis. Even if the incident heat flux on the sample surface is same in both the tests, the amount of heat flux absorbed differs depending on the absorptance of the sample and the wavelength of radiation emitted by the heater. To produce the same amount of heat flux, the tungsten lamps need to be on higher temperature than the electrical heater in cone

calorimeter, which results in the variation of emitted radiation wavelength. After testing wood and PMMA in both the apparatus, it has been found that for both samples, absorptance is relatively low in the operating wavelength range of tungsten lamps (<2 μm) and high for the range of conical heater (2 μm). It was also noted that both samples absorb most energy when it is radiated at wavelengths higher than 2 μm (Girods *et al.*, 2011; Karyaparambil, 2017).

When PMMA was exposed to the tungsten lamps, it was noted that the mass loss rate is lower since wider energy distribution occurs within the sample while the energy absorbed remained low. Higher mass loss for samples exposed to conical heater is a consequence of higher quantity of energy absorbed and it is not dependent on the thickness into which the energy is distributed (Girods *et al.*, 2011; Karyaparambil, 2017). So, depending on the absorptance of pine needles, the FPA may have been underestimating the results so far.

In conical heater, the sample is directly under the heater and the radiation is incident on a wide range of angles due to the conical shape, whereas while using tungsten lamps in FPA, the incident radiation is between 70° and 80° to the normal of the sample surface. This variation results in a reflected ratio of radiation between 0.17 and 0.39 (Girods *et al.*, 2011; Karyaparambil, 2017). The incident angle may also have an impact on how the re-radiation occurs inside the 0% porous sample holder which is lined with aluminium foil. The re-radiation intensity could be higher than for cone heater where the intensity of incident radiation is spread across a wide range of angles.

Cone calorimeter is a multi-variable test and readily offers parameters required to analyse wind-aided flame growth. But since the sample is placed on the weight gauge it adds additional radiation on the sample reflected from the base of the gauge and prevents air flow from bottom. The presence of the load cell preventing air flow from the bottom and not being able to regulate the air flow had been the main reasons why previous tests favoured FPA over the cone

calorimeter. However, for this test, a modified sample support as shown in Figure 8 was used to allow air flow from all sides and tests are only done under natural convection.

Figure 8: Sample on the improvised sample supporter used to enable adequate air flow through the bottom of the sample.

Fire safety engineering and fire modelling largely depend on the flammability characteristics of materials obtained from such tests which makes them crucial for the field. These parameters can be used to predict the height of the flame, potential for flashover, etc. (Drysdale, 2011). Ignition test in cone calorimeter seems to be more reliable in a well-ventilated fire as the cone offers better view factor and wavelength absorption properties than the lamps in FPA. Since in this experiment, only natural convection is being tested for and since critical heat flux is the point of focus, it was decided to choose cone calorimeter instead of FPA.

3.1.1. Cone Calorimeter

Cone calorimeter (Figure 9) is a versatile apparatus that works on oxygen calorimetry, the principle that the net heat of combustion is proportional to the oxygen consumed in the process (approx. 13.1MJ/kg of O_2 consumption). The contribution by the product under test to the rate of heat evolved during a fire is assessed with this method, along with the smoke production rate in a well-ventilated fire by *Bouguer's law*. Heat release rate, mass loss rate, time for ignition, smoke production rate, critical heat flux, amount of oxygen consumed, gas analysis, are among the data obtained from the test (Lindholm et al., 2009; BS ISO 5660-1-2015, 2015).

The equipment consists of a cone-shaped radiant electrical heater, radiation shield, irradiance control, weighing device, specimen holder, retainer frame, exhaust gas system with flow measuring instrumentation, gas sampling apparatus, ignition circuit, ignition timer, oxygen analyser, heat flux meters, methane calibration burner used to calibrate heat release rate, smoke obscuration measuring system, smoke system thermocouple and optical filters (BS ISO 5660-1-2015, 2015; Karyaparambil, 2017).

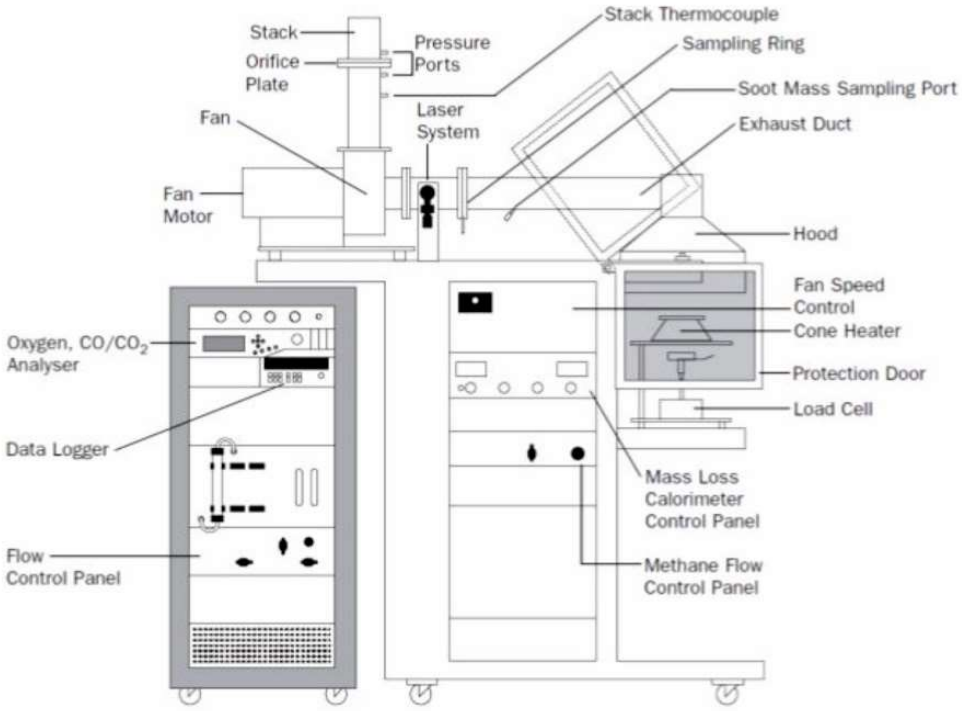

Figure 9: Cone Calorimeter (Lindholm et al., 2009).

Prior to tests, calibration is done as per (BS ISO 5660-1-2015, 2015)(10.2) and ensured that the test environment is as described in (BS ISO 5660-1-2015, 2015)(9). Baseline data is collected for 60 seconds prior to ignition and experimental data is then measured from this baseline data. Once the specimen is prepared, it is placed on a metal sample holder and then the holder is placed on a load cell which measures the weight of the sample throughout the test. The standard sample should be of the size 100 mm x 100 mm with a maximum thickness of 50 mm and wrapped by aluminium foil to ensure that heating only takes place on the top and not on the sides. Once the required heat flux is achieved at the water-cooled heat flux meter at 25 mm below the cone by adjusting the conical heater, it is replaced by the sample placed at 25mm below the heater. Just above the sample, below the cone surface, a spark ignitor is situated which ignites the flammable gases from the sample surface. Times at which initial flashing and transitory flaming occurs is noted. The experiment is repeated on three more specimens for accuracy. Although the standard test is carried out in horizontal alignment, a vertical alignment is also possible with necessary adjustments (Lindholm et al., 2009; BS ISO 5660-1-2015, 2015; Karyaparambil, 2017).

The extraction hood above the heater collects the flue gases from the burning and gives data on the combustion gases produced. The filters inside removes particles and moisture and a laser photometric beam measures the amount of smoke produced.

3.2. Sample Preparation

It is necessary to have a good test sample to get a reliable result from the experiment. The samples used in this test were pitch pine needles filled in 63% porosity cylindrical sample baskets of the size 130 mm (diameter) by 30 mm (height). This sample basket was selected to allow adequate natural convective flow through the sample while having a circular sample to match the circular heating profile of the conical heater being an added advantage. The results from tests using this sample basket could also be compared with the previous experiments done with FPA and could be helpful in comparing future experiments on porous fuel bed which may use a similar sample basket.

The porosities studied in this thesis were selected to match tests in Ravena, (2019) and 94%, 90% and 85% porosities were selected, which would account for 15 g, 25 g, and 35 g pine needles in the sample baskets before drying. Different porosities were achieved by changing the density of the sample. A sample with higher density will have more needles in the same volume and thus less air gaps or pores in it.

Care was given not to damage the needles while packing and yet they were packed with a good amount of randomness. While 94% porous sample could be made with pine needles in their natural form, 90% and 85% samples were prepared by cutting the needles to smaller sizes. They were cut into pieces of about 3 cm in length. While they could be just dropped into the sample basket to prepare 90% sample, some pressure had to be applied to pack them in 85% porosity.

The samples were prepared by avoiding damaged or disoriented pine needles as much as possible. However, it should be noted that there may be some unevenness inside the bulk bed. Since the needles kept moving out through the holes in the basket, the baskets were covered in aluminium foil before filling the needles and removed just before the test. The mass of the basket covered in aluminium foil, with and without needles were noted. The samples were packed to the brim of the sample basket before drying and they were placed inside an oven at 60^{o}C for 24

hours. While in the oven, a porous sample basket with a flat bottom was placed on top of the sample to make the surface of the pine needle bed relatively flat before the test. For 85% porous samples, a weight was put on the porous sample basket on top to make sure they fit well inside the basket once dried.

Moisture content

Fuel moisture content and the influence it has on the result is not looked upon in this study due to limitation of time. The sample is dried for 24 ± 1 hours before the test and is made to rest in ambient temperature for one hour before testing. Hand gloves were used while handling the samples to prevent any moisture being transmitted to the samples while handling. The samples were taken out at least one hour before the test, weighed and allowed to cool. The samples were weighed again before the test to note the amount of moisture regained by the pine needles while it was outside the oven. It was assumed that the difference in SVR due to drying is negligible.

It was observed that about 0.99% of the dry mass taken out of the oven was regained before the experiment as moisture. On an average 1.19 g moisture was removed before test from 15 g (94% porous) sample, while ≈1.8 g was removed from 25 g (90% porous) sample and ≈x g was removed from 35 g (85% porous) sample.

A consistent 60-66% increase was observed in the increase in moisture removed which was almost consistent with the increase in mass of the sample being dried according to different porosities.

One of the most important part fact about this experiment is that it was done using a porous sample basket and a porous sample holder under cone calorimeter. The porous sample holder allowed airflow from beneath the sample. It was made from two sample baskets jammed together as shown in Figure 10. This sample holder had a slightly smaller openings in the top than 63% opening in the sample basket itself. However, in the bottom, the opening was like that

of the sample basket. The effects of this difference were ignored. Figure 11 shows the sample baskets filled with needles for different porosities.

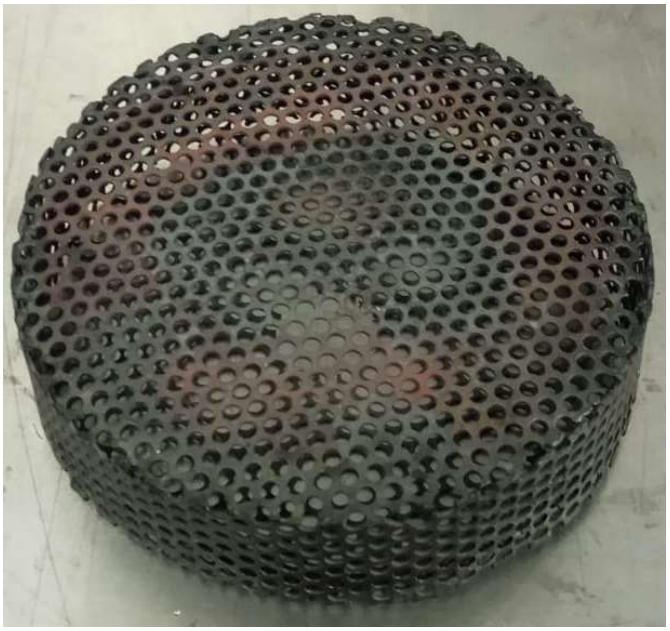

Figure 10: Sample supporter. A combination of two sample baskets mounted against each other.

Figure 11: Samples of 94%, 90% and 85% porosities. First sample is ready for test. Second is while the aluminium foil is being removed and third is just when it was taken out of the oven.

3.3. Experimental procedure in Cone Calorimeter

This section describes the entire experimental procedure adapted for this study in detail keeping in mind that at some point anyone interested could redo the experiments.

The exhaust air flow was kept at around 24 L/s, the gas analyser in the cone calorimeter was calibrated and the cone height was adjusted so that the surface of the sample was 25 mm below the cone. The temperature corresponding to the desired heat flux was set at the cone calorimeter temperature control and an average heat flux was measured using the record function in the interface. Temperature of the cone was calibrated using the heat flux gauge before each test to avoid miscalculating the incident heat flux due to any aberrations in the cone. It was ensured that the heat flux gauge was positioned in the same location each time by fixing it using the gauge holder in the cone and keeping it in-line with the edge of the holder. The gauge was fixed at the same distance from the cone that the surface of the sample was fixed.

The heat flux gauge was removed, and the sample was inserted with a sheet of aluminium foil on top of it so that the heat from the cone is restricted to an extend from reaching the sample. The test was started as soon as the foil cover is removed. Figure 12 shows the test setup inside the cone calorimeter test chamber and Figure 13 shows the test setup.

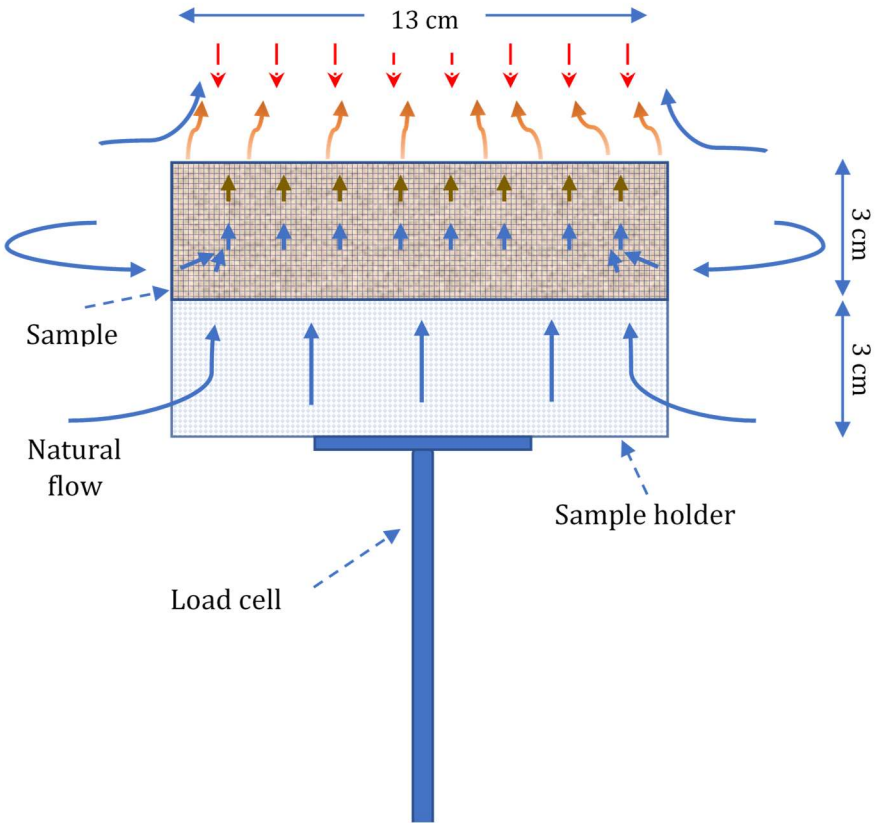

Figure 12: Diagram of the experimental setup

Figure 13: (Left) Test setup. (Right) Visualisation of samples lifting up while burning.

The sample was observed throughout the test to understand the behaviour of the sample under the exposure to heat flux and to note the time to ignition. By minimising the variables in the test, the only existing variables will be those in the sample itself, which could not be controlled.

If no ignition was observed, another sample was tested with a heat flux 1-2 kW/m^2 higher than the initial heat flux, while if ignition occurred, a lower heat flux was tested until the critical heat flux was found., each time using a new sample. If there was no ignition at a value X, but there was ignition at A (A=X+0.5 kW/m^2), then A is taken as the critical heat flux and no values between A and X were tested for. At least two tests were done to verify the critical heat flux.

The sample with the same porosity was then tested once for heat fluxes 20, 30 and 40 respectively to find the time to ignition which is then plotted in a graph with $1/\sqrt{t_{ig}}$ and the critical heat flux, where t_{ig} is the time to ignition. The results from these tests need to be treated with caution as only one test was done for each external heat flux 20 kW/m^2 and above.

The test was then repeated for samples with different porosities.

Flow/No flow conditions

The impact of cooling from the airflow through the samples was studied by testing two samples of 94% porosity, packed at the same time and dried for the same duration, with one being wrapped in aluminium foil around it and the other packed into 63% sample basket as usual. They were tested under 20 kW/m^2 heat flux.

This test was expected to help to understand the dependence of airflow through the sample on time to ignition by using open and closed baskets. The effect of flow was attempted to be distinguished from the effects of SVR and charring of surface layer the since they were expected to stay similar.

4. Results & Discussion

The data analysed were collected from the excel sheets produced by each experiment and from visual observation of the sample throughout the test. It should be noted that there could be errors within the operational software of the cone calorimeter and the gas analyser which would have produced caused errors in the data obtained.

Some of the most important parameters that would affect the variation in time to ignition and critical heat flux are the cooling effect from the natural convective air flow through the sample; rate of pyrolysis gas production which would affect the time to ignition; exposed surface area of sample resulting in changes in radiative heat transfer and in pyrolysis gas production; the charring of top layer of the needle bed creating a barrier so that the needles below that layer are prevented from pyrolyzing. In this section, it was attempted to separate other effects from convective cooling.

4.1. Ignition behaviour

The expectation was that as porosity of the sample is increased, the void spaces in the fuel bed increases and this would increase the permeability of the sample which would increase the flow of air through the sample. If there is more flow, the air would cool the pine needles being exposed to the external radiation and the layer of pine needles beneath the exposed layer. If the heat energy being transferred to the pine needle is not higher than the critical temperature below which the rate of pyrolysis gases will not result in a flammable mixture, it would prevent ignition under that specific heat flux. There may still be pyrolysis happening, but the rate of pyrolysis may be too low to form fuel-air mixture in the flammability range. In other words, the heat losses due to convective cooling and radiative losses will be more effective than the heating due to external heat flux (Thomas, 2017). The heat flux must be increased to supply more energy to the pine needle to overcome the threshold temperature to increase the pyrolysis rate.

In total 52 tests were done for the three different porosities under different external heat fluxes and the times to ignition for corresponding heat fluxes are shown in Table 4. It should be noted that the mass of sample after combustion was measured and found to be too small and too sensitive to make any proper conclusion. Since some pine needles fell out through the pores of the sample basket during combustion, the value measured may not be useful at all. So, any mass related measurement is to be treated with caution.

Table 4: Time to ignition and corresponding external heat fluxes for different porosities

15 g - 94% porosity		**25 g - 90% porosity**		**35 g - 85% porosity**	
$\dot{q}''_{ext}$ **(kW/m2)**	t_{ig} **(s)**	$\dot{q}''_{ext}$ **(kW/m2)**	t_{ig} **(s)**	$\dot{q}''_{ext}$ **(kW/m2)**	t_{ig} **(s)**
19.5	118	17	183	14	151
19.5	125	17	173	14	143
20	96.33	17	79	14.5	139
20	89.23	17.5	69	15	119
30	11	17.5	77	17	35
40	5 (4-6)	18	43	20	22
		20	27	30	10
		30	10	40	5 (5-6)
		40	5 (5-6)		

Although the incident radiation will be on a circular plane on the surface of the sample, it did not cover the entire sample surface itself. Only a portion of the surface has the high intensity impact of the radiation as shown in Figure 14. The rest of the sample surface may pyrolyze in a different rate compared to the exposed surface.

Figure 14: 85% porosity at 13.5 kW/m² (Area towards the edges are not charred)

Intense production of pyrolysis gases was observed as soon as the test was started in almost all tests. But it stopped soon, and a char layer was then formed on the exposed surface. While observing unburned samples, it was also observed that a layer of charred needles was formed in the exposed surface of the sample. A trend of increased layers of charred pine needles was observed in the unburned samples as the porosity of the sample was reduced. But the depth of charred layer was smaller for lower porosity (or higher density) samples than for a more porous sample. This was in accordance with the theory explained in Section (2.1.1.1). It was also observed that some needles tend to have moisture on them while being exposed to radiative heat flux from the cone heater. The presence of moisture would have acted as a heat sink which also would have helped to cool down some of the needles further. However, this effect has not been further explored.

It is important to note that in this thesis, the critical heat flux ($\dot{q}''_{crit}$) was considered as the "minimum heat flux for ignition, ($\dot{q}''_{min}$)", which is the minimal heat flux below which no ignition for that specific sample, under practical conditions would be possible. As predicted, there was

a change in critical heat flux observed with the change in porosity of the fuel sample bulk as shown in Figure 15. Only three porosities were tested for and this does not give the full picture of the relation. Although the relation seems linear, it is applicable only in the range of porosities tested for. There may be a species dependency on the result which was not studied in this report.

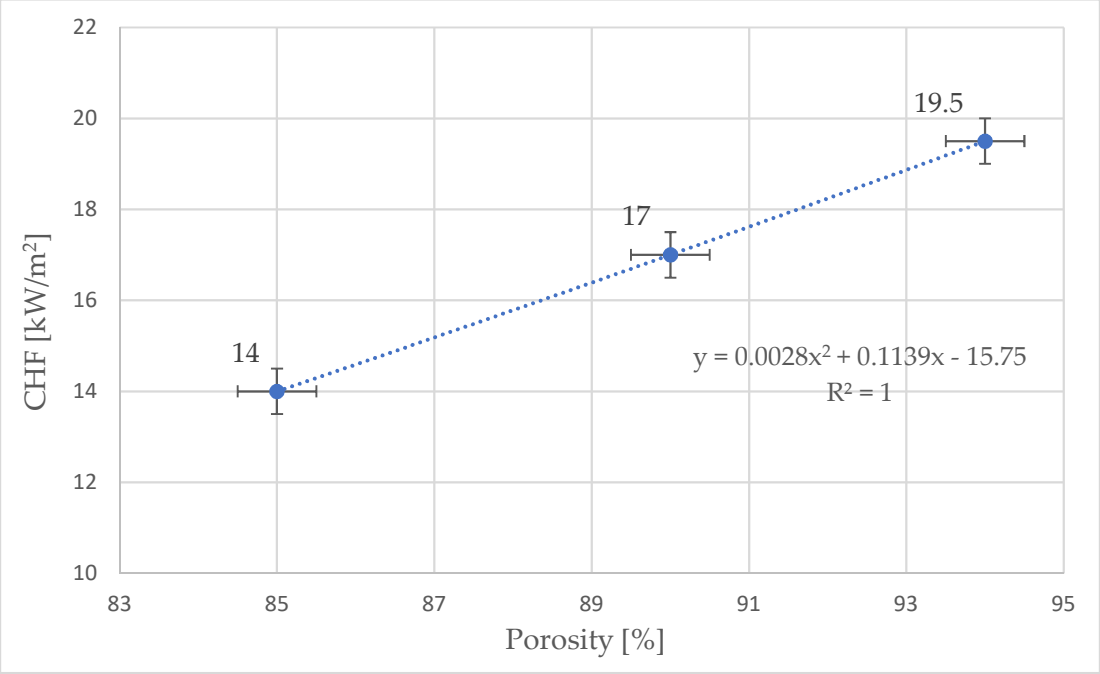

Figure 15: Critical heat flux vs Porosity of fuel sample bulk.

Time to ignitions for 85% and 90% porous samples were quite similar compared to each other with a difference less than 10s. It must be treated with caution since only one test was done for each porosity under 20 kW/m². Similar times of ignition may be explained by similar surface to volume ratio resulting in similar pyrolysis rates, while porosity acting against the effect by introducing more convective cooling in 90% porous samples.

Ravena, (2019) had found that at 85% porosity, the samples exhibited the least times to ignition compared to porosities lesser or greater than that. It was attempted to create a sample with 75% using 63% open baskets and it was not successful as the needles kept falling out of the basket

before test and since great pressure had to be applied on the samples to compress them and fit them into the sample basket.

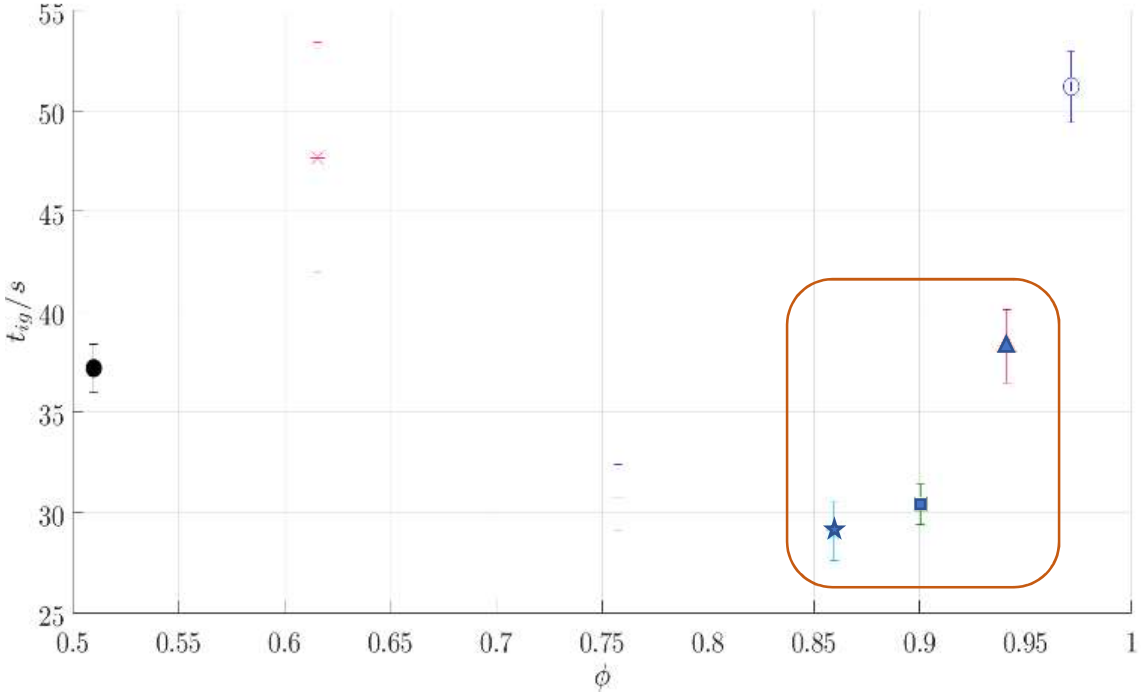

Figure 16: Time to ignition vs Porosity (Ravena, 2019)

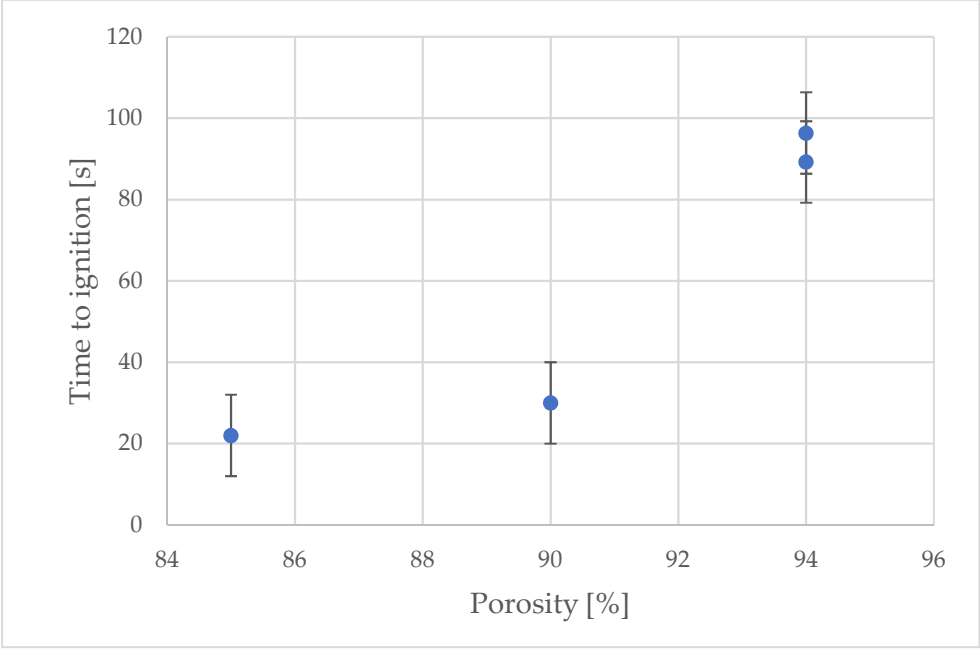

Figure 17: Time to ignition vs Porosity

Ravena, (2019) also found an increasing trend in time to ignition for the same porosities (85%, 90% & 94%) as shown in Figure 16. As shown in Figure 17, a similar trend was observed while plotting the time to ignition for the new experiments as well. Although the trend is similar, the values are quite different. It could be observed that at 90% and 85% porosity, although closed baskets were used, Ravena, (2019) still got a higher time to ignition compared to tests done for this thesis. This behaviour may be due to two factors, usage of a different testing apparatus and the number of tests done. As explained in Section (3.1), the radiation absorption properties of pine needles to the wavelength emitted by the tungsten lamps in FPA may be weaker compared to the radiation emitted by the electric cone heater. Therefore, the spectral properties of the high temperature lamps may be one of the reasons why there is a higher time to ignition under a higher external heat flux (25 kW/m^2) for the same porosity samples. The other reason for this difference in results may be due to the number of tests done by Ravena, (2019). The results shown in Figure 17 was the result from just one experiment.

Although Santoni *et al.*, (2014) found an increase in energy released with increasing porosity, they concluded that it does not affect the times to ignition, which is contradictory to the results observed in this thesis.

Figure 18 shows the graph with times to ignition for different porosities plotted against the external heat flux applied. The lines drawn to the asymptote shows the minimum heat flux of ignition which in this case, may be considered as $\dot{q}''_{crit}$. It could be seen in Table 4, for 90% porosity time to ignition varied across an extensive range for the same heat flux (17 kW/m^2). This may be partly explained by the rapid change in t_{ig} values close to the $\dot{q}''_{crit}$ where $t \to \infty$. However, this may still not explain why when it comes to values close to $\dot{q}''_{crit}$ 94% and 85% sample follows a similar trend, but 90% samples do not. It could be seen that while t_{ig} under $\dot{q}''_{crit}$ for 94% porous sample was 118-125s while for 85% porous sample, it was 143-151s. The value

expected for 90% porous sample should be between these two ranges. However, the range varied between 79-183s. Due to time restrictions, more tests to verify this was not done.

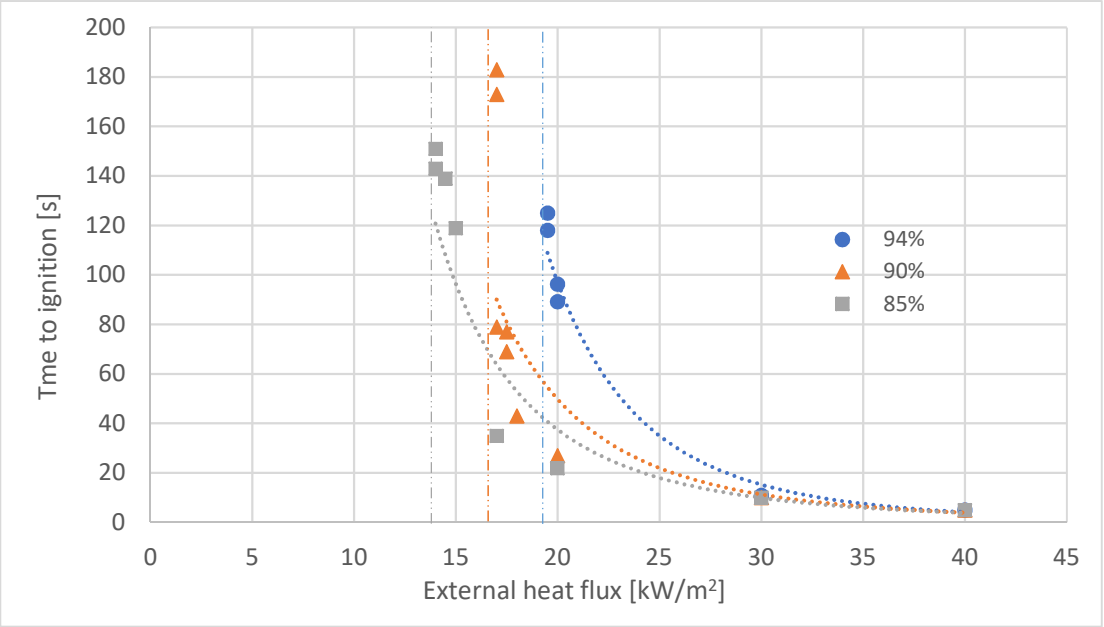

Figure 18: External heat flux vs time to ignition for different porosities.

The values were plotted in a graph with external heat flux against $1/\sqrt{t_{ig}}$ as shown in Figure 19 since the typical ignition theory of solids states that for thermally thick materials, time to ignition is proportional to one over the square root of the external heat flux (Quintiere., 2006; Torero, 2016; Thomas, 2017). But Thomas, (2017) concluded that the sample beds behave as thermally thin below 60 kW/m² but it was decided to treat the sample as thermally thick for the ease of analysis although trying to understand the graph based on solid ignition theory may not give reliable results. The graph was still used to understand the deviation of the pine needles from a thermally thick samples and to see how much they match the convectional theories. It may be seen that when the trendline is extended to the origin of the graph, only 85% porous samples seems to follow it to some extend.

It was observed that the effects of porosity become irrelevant as the applied external heat flux is really highand that it plays a role in ignition behaviour when the external heat flux is more closer to the critical heat flux. The 4-6 second time to ignition as observed for almost all the samples

under 40 kW/m² was mostly the delay time for the pilot spark to move on top of the sample and start the pilot spark. There was ignition almost instantaneously as the spark started.

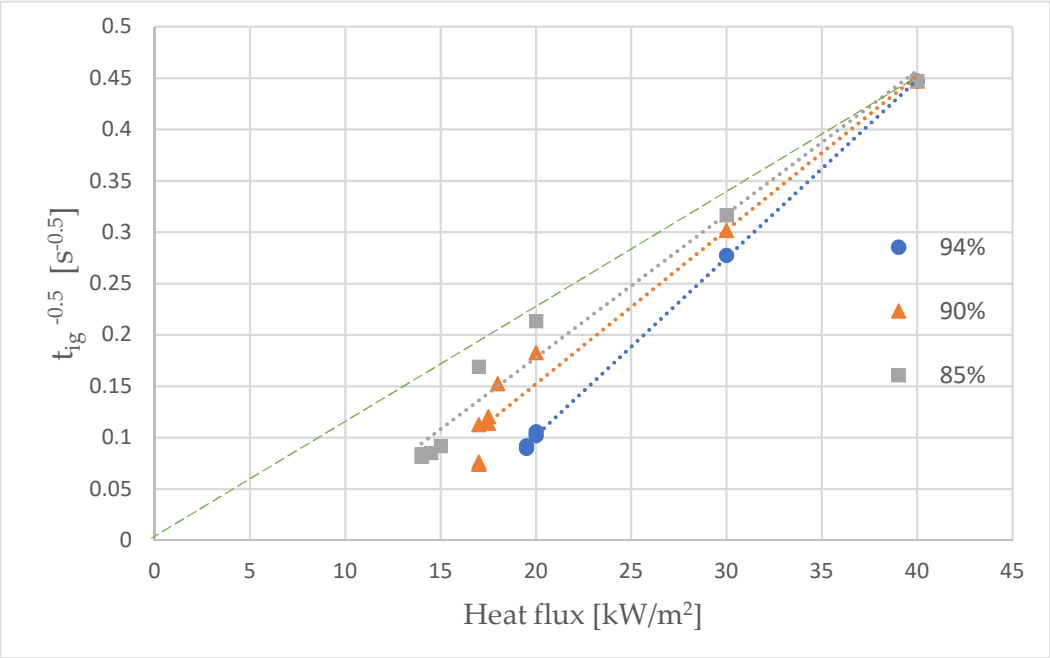

Figure 19: External heat flux plotted against inverse square root of time to ignition (without error bars).

Table 5 shows some of the main experimental results as was observed. However, it should be noted that while changing the porosity, we are also changing a lot of other parameters as discussed in Section (1.1). The presence of these dependent variables (and any unknown confounding variables) make the data questionable as to which parameter contributes to which effect. We could try to eliminate as much variables as possible and try to analyse the data to see how the results depends on them, but still, due to the uncertainties linked with the analysis, the experiment and the data collection, one should be cautious about the reliability of the results.

Table 5: Results

Sample Porosity	**Critical Heat flux (kW/m²)**	**Peak HRR under 20 kW/m² (kW)**	**Time to Ignition under 20 kW/m²(s)**	**Avg. Pyrolysis rate under 20 kW/m² (g/s)**	**Avg. Sample Density (kg/m³)**	**Test series**
94%	19.5	8.65	89 –96	0.0066	34	1-25
90%	17	5.84	27	0.0239	58	26-40
85%	15	4.74	22	0.0255	81	43-51

4.2. Post-Ignition

One of the most important post-ignition observations was the difference in heat release rate with porosity. There was a trend of reducing peak HRR and increasing flameout time with reducing porosity of the samples as shown in Figure 20.

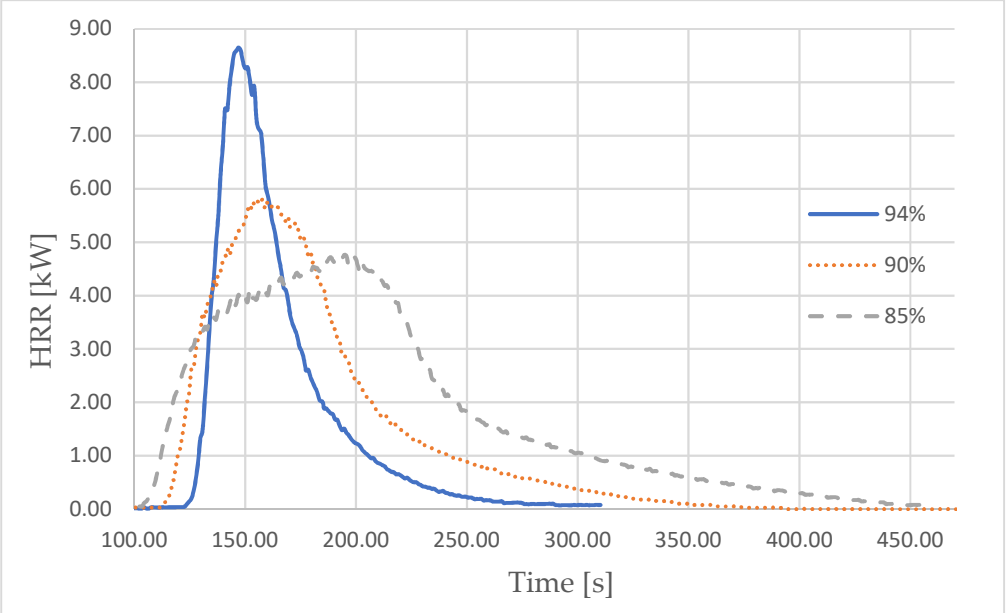

Figure 20: HRR over time for different porosities under 20 kW/m².

It shows clearly how less porous sample ignited first and the most porous one ignited the latest. While there was a fast fire growth for high porosity samples, low porosity sample had slower fire growth, but it burned for a longer time. The area under the curve was found and the total heat released by each sample was analysed and tabulated as shown in Table 6. It was found that the efficiency of combustion increased with increasing porosity. This is no surprise since although in 85% porous sample, more fuel is available which reduces the amount of air flow through the sample supplying oxygen to the combustion zone. Thomas, Hadden and Simeoni, (2017) had studied the impact of oxygen flux on burning dynamics of forest fuel beds and found that the combustion efficiency decreased when oxygen entrainment was restricted. El Houssami *et al.*, (2016) and Bartoli *et al.*, (2011) had also arrived at a similar conclusion that bigger voids in the fuel bed allowed more oxygen to pass through it and it contributed to more energy release

than a fuel beds with less voids in it. Howard, (1971) found that the heat of combustion for some pine needles were around 21 MJ/kg which is much less than the value found here.

Table 6: Total heat released for different porosities.

Porosity	Total heat released (kJ)	Mass burned (g)	$\Delta H_{c,eff}$(MJ/kg)
0.94	349	13.79	25.3
0.90	472	23.18	20.36
0.85	642	32.44	19.79

However, as stated in Santoni *et al.*, (2014), a high SVR could also contribute to increased combustion efficiency and HRR. Since the needles had been cut down into pieces for 90% and 85% samples, they would clearly have a lower SVR than 94% samples since the permeability of the 94% sample would be higher which would generally mean that it has a higher exposed surface area. So, the lower combustion efficiency in less porous samples may be either from the effects of SVR or airflow through sample bed.

To separate the effects of SVR and charring depth (restricting pyrolysis) from the effect of convective cooling, acted as the motivation in doing tests with open and closed baskets with same porosity under the same external heat flux. Comparison of HRR with time for both tests are shown in Figure 21. There are clear differences in the result which shows a dominating impact of airflow through the samples.

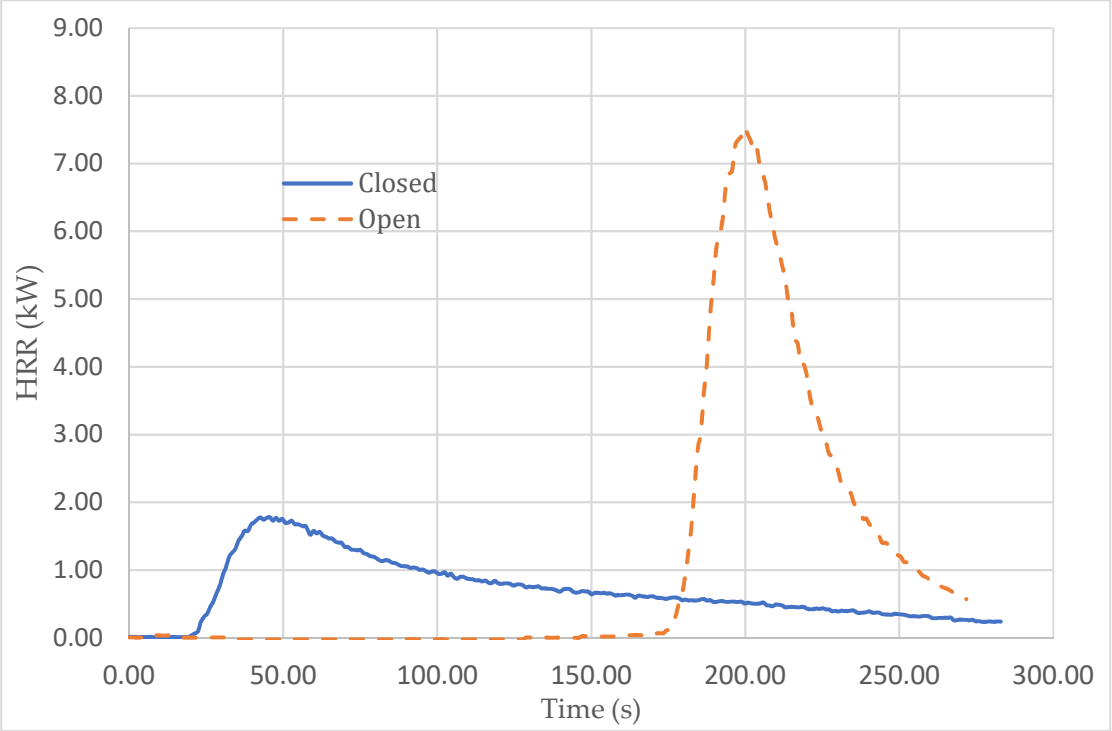

Figure 21: Open and closed basket comparison at 20 kW/m².

There is a considerable increase in time to ignition (170s) for open basket compared to a closed basket (25s). As stated in Table 7, the average mass loss rate before ignition between start of test ang ignition for closed basket condition is twice as much as for open basket. However, it may be argued that the pyrolysis gases that may indeed make an impact in ignition are the gases produced a few seconds before ignition. So, the mass loss rate (or pyrolysis rate) for the last 5 seconds were considered and it was found that the value for open basket test is twice as more than closed basket. This may be explained by longer exposure to the radiative heat flux of open basket compared to closed basket, raising up the bulk temperature gradually but still being influenced by the convective cooling which slows down the pyrolysis rate till ignition. If a thermocouple had been installed inside the samples to measure the temperature inside it just before ignition, the value might have been higher for open basket compared to the closed basket. In short, when the closed basket ignites, the pyrolysis gases that may be contributing to ignition comes mostly from a thin layer beneath the exposed surface while in case of open basket, it could

be produced by a thicker portion of the fuel bulk as they are all at a higher temperature while the cooling effect may gradually have been limited to the sides and bottom of the sample.

Table 7: Open and closed basket results.

Condition	Ignition Time (s)	Peak HRR (kW)	Average MLR before ignition (g/s)	Average MLR 10s before ignition (g/s)
Closed	25	1.74	0.014	0.0098
Open	170	7.54	0.007	0.0197

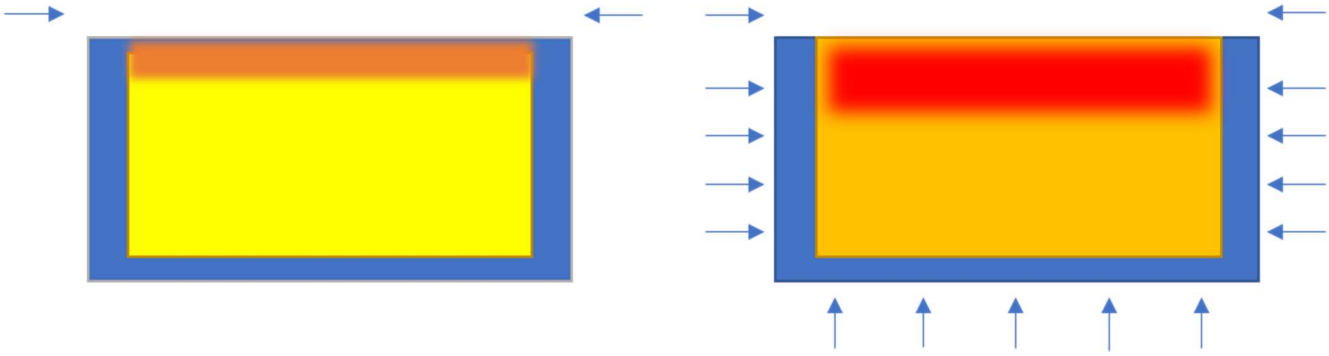

Figure 22: Visualisation of thermal conditions inside the closed basket sample (Right) and open basket sample (Left)

Figure 22 helps to visualise the thermal scenario inside the samples. In a closed basket, although the temperature on the surface may be high enough to cause enough pyrolysis, it may not be that high and the bulk below that surface will have heated up to a much lower temperature since the exposure time before ignition is much smaller compared to the open basket sample. So, there is not enough time to heat up the entire bulk. However, for open samples, the exposure time is higher which gives enough time for the bulk to get heated up to a higher temperature than the closed basket. The gradients formed inside the fuel bed may be visualised with the help of Figure 23 where El Houssami *et al.*, (2016) shows the numerical predictions and experimental results for the temperature evolution in depth, at different positions in the sample, for different times of exposure.

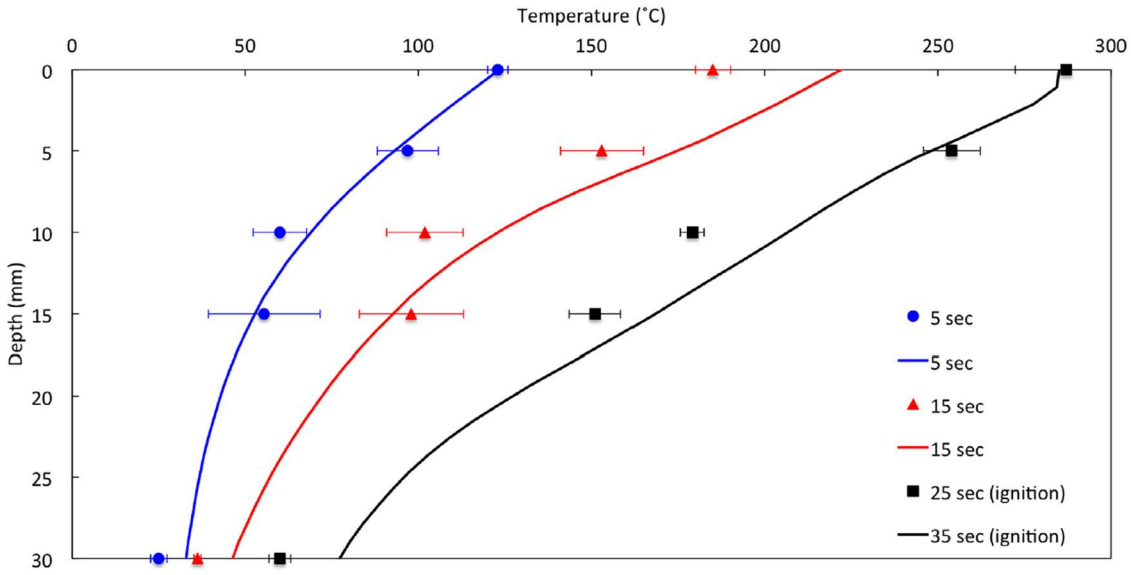

Figure 23: Temperature profile before ignition for pitch pine, bulk density of 40 kg/m3, 25 kW/m2 applied heat flux. Symbols: Experiments, lines: Simulation. (El Houssami et al., 2016)

However, this explanation is valid mostly if the sample basket is behaving as a homogenous porous bulk. But since this may not be the case, it may have localised cooling and localised heating effects along with dilution of pyrolysis gases keeping them below lower flammability limit.

Such a big difference in ignition times even when all the other properties of the samples were kept similar could be explained by the presence of convective cooling along with some other effects. There could be re-radiation occurring from the aluminium foil heating up the whole fuel bulk and producing a lot of pyrolysis gases which results in a faster ignition. But in the previous paragraphs, it was explained that the pyrolysis rate that lead to ignition was lower than that for open basket. Besides, the external radiative heat flux applied is already high at 20 kW/m^2. It is dubious that the re-radiation would make any considerable impact compared to the external radiation. Therefore, the only effect that may dominate is the convective cooling itself. Since the convective flow into the fuel bed could occur from all sides, the dynamics inside the fuel bed is quite complex to understand or make a model for. There will be cold air moving in from the

bottom and the sides of the sample which are driven by the heating of air above the sample and the heated air moving up which creates a form of buoyant suction on the surface.

The HRR results for open and closed basket matches with the trends observed by Thomas *et al.*, (2014) when they tested different condition for *Pinus rigida.* The closed basket sample had a longer flaming time but very low peak HRR compared to the open basket sample. It could only be explained from the increased combustion efficiency from the airflow through the samples, supplying more oxygen to the combustion zone. However, they had also stated that there was no considerable difference in ignition times between open and closed sample baskets under natural convection which was contradictory to the results found in this thesis.

However, the post-ignition dynamics of the pine needles is difficult to study with cone calorimeter as the pine needles tend to show a level of cohesion between each other while burning and deform as a bulk. They lift and moves closer to the cone as shown in Figure 13, which brings about a whole different combustion and convection scenario which would be complex to study.

The heat energy incident on the fuel surface will be different at different parts of the surface. There was a layer of char on the surface of the samples and smouldering beneath it. It was observed that flaming mostly occurred from around the sides. The shape of the flame may be due to the buoyancy created by natural air flow and the exhaust hood. Airflow will be happening to the inside of the sample from all sides and the bottom of the sample basket, which along with the suction airflow in the hood and the cohesion between burning particles, may be responsible for this behaviour.

According to Babrauskas, (2016), a gauze is kept on top to prevent intumescence of samples influencing the combustion dynamics. However, no such measures were taken in this test since it was assumed that it would act as a heat sink or will affect the free combustion behaviour of

pine needles. This may be considered as one of the limitations of the study done in this thesis on post-ignition characteristics.

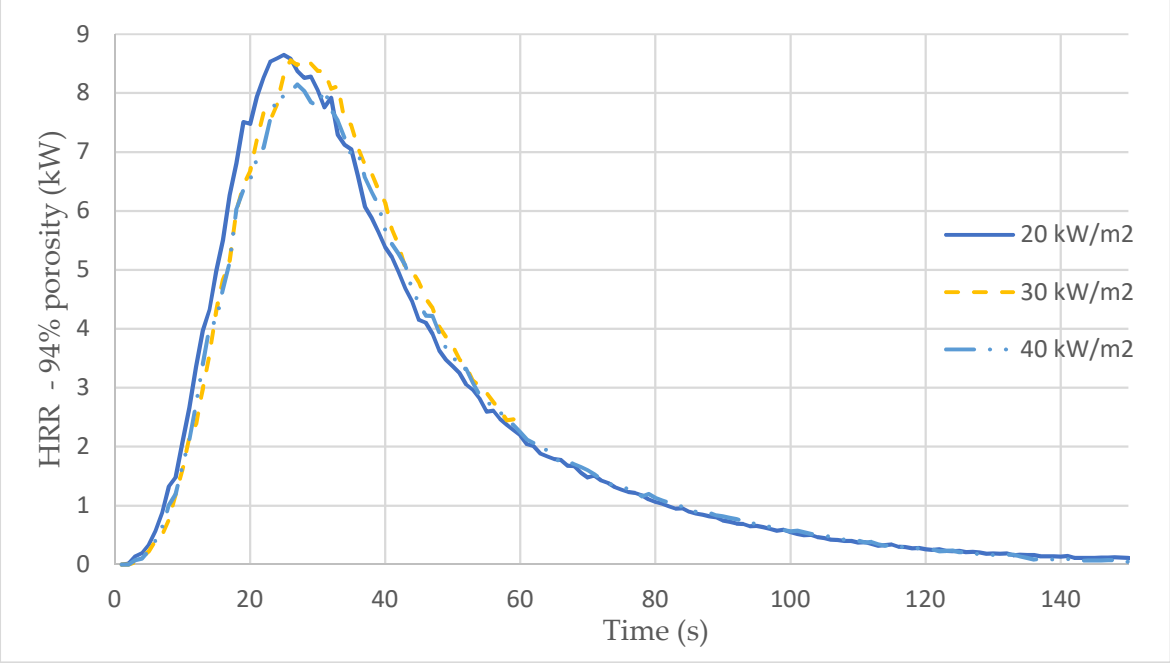

Figure 24: HRR with different heat flux for 94% porosity sample.

While analysing the HRR for different external heat fluxes for the same sample, it was found that the HRR did not differ much with external heat flux as shown in Figure 24. One would expect a higher HRR with increasing external heat flux as more heat is available to cause increased pyrolysis. However, the results from this study shows that it the bulk properties of the fuel sample that decide the heat release rate and not the external heat flux. This shows the importance of bulk properties in studying wildland combustion behaviour. It should also be noted that the results in the graph are from one test done for each heat flux and considering the complexities of wildland fuels, more tests may be required to obtain a more reliable data.

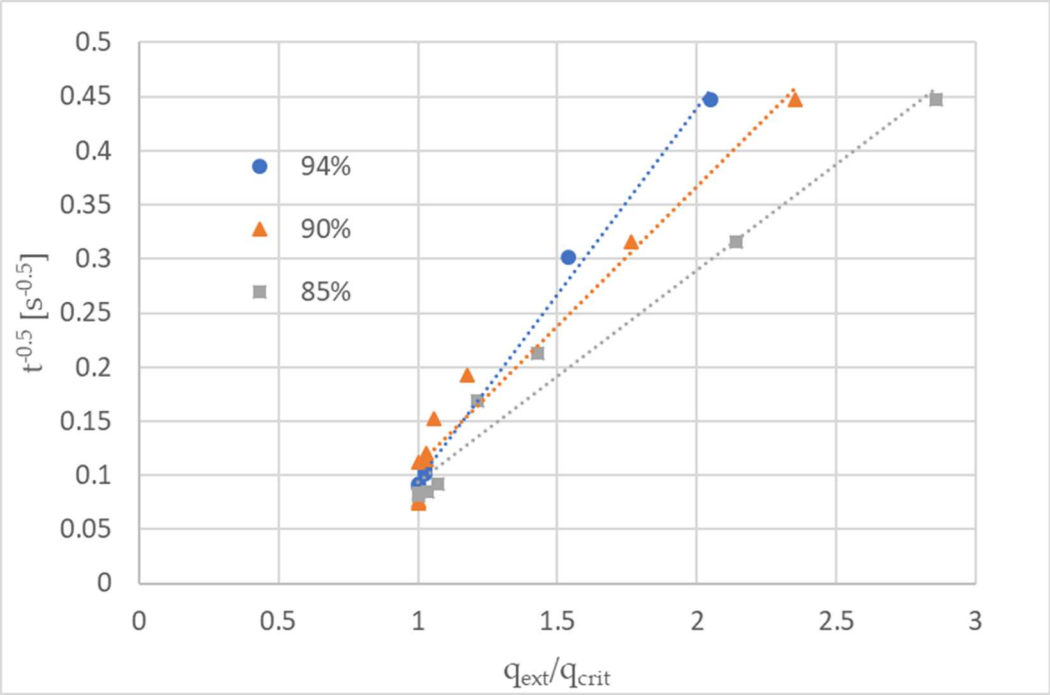

Figure 25: Thermal inertia analysis

It was attempted to see the behaviour of thermal inertia ($k\rho c_P$) of the sample bulk and the graph as shown in Figure 25 was made. The slope of the lines must represent the thermal inertia as per the equation

$$\frac{1}{\sqrt{t_{ig}}} = \frac{\pi}{k\rho c_P}\left(\frac{\dot{q}''_{ext}}{\dot{q}''_{crit}}\right)$$

which was derived from the equation,

$$\frac{1}{\sqrt{t_{ig}}} = \frac{2}{\sqrt{\pi}}\frac{a}{k\rho c_P}\left(\frac{\dot{q}''_i}{T_{ig} - T_\infty}\right)$$

which is used for thermally thick samples. The differences in slopes for different porosities show that the thermal inertia of the sample varies with porosity. Since porosity changes the sample density, the effect could be directly influencing the thermal inertia which is a function of density.

5. Conclusion

The relationship of porosity of pine needle bulk to the critical heat flux of ignition was experimentally analysed in this thesis. Although wildland fuels are complex to characterize and compare with convectional fire test samples, it was still possible to obtain relevant results while comparing samples within themselves. The critical heat flux of ignition was found to increase linearly with increasing sample bulk porosity. It should be noted that the relation may be valid only between the ranges of porosities (85%-94%) tested. There may also be strong dependence towards the species of pine needle tested and fuel moisture content of the needles, which was not studied in this report. The effects of other dependent variables were separated from that of porosity by doing tests with open and closed sample baskets which showed significant reduction in time to ignition when the airflow through the sample was restricted. The effects of re-radiation from the aluminium foil was assumed to be insignificant considering the high heat flux to which the samples were already being exposed to. Further researches with a different covering material may be carried out to verify if re-radiation does make any difference. Once ignited the open sample basket had a much higher peak heat release rate and better combustion efficiency than the closed basket sample.

The presence of impurities, decayed needles and thin strands of needles influence the ignition results. Impurities may delay or accelerate ignition process depending on the type of impurity, while decayed or thin strands of pine needles may undergo smouldering before the other particles and cause an early ignition which may not be the realistic ignition time if that specific needle was not present. But it could be argued that there exists a high level of uncertainty and randomness associated with wildland fuels that may make the presence of such impurities and imperfect fuel particles, quite insignificant.

Deformation of the pine needles when exposed to the radiant heat is an unavoidable issue which should be acknowledged. The needles tend to bend in the presence of heat and this had caused many false ignitions during the experiments when the needles bend towards the pilot flame and

got ignited directly. Deformation of the fuel bulk while burning should also be acknowledged. The needle bulk, rising above the sample basket towards the cone heater would clearly result in combustion behaviour which would give deceptive results.

One of the notable issues which would decide the ignition times is the presence of pyrolysis gases close to the pilot spark. If the heat flux is high enough, pyrolysis gases may be produced, which, when within flammability limit, can get ignited. However, if the gases are produced or present away from the pilot spark, it will not get ignited. The presence of pyrolysis gases over the sample bed would depend on the structure of pine needles.

It was observed that some needles get pushed out of the sample basket through the sample basket pores while the surface is being deformed by the external heat flux. As discussed earlier, this loss of mass would influence the mass calculations and give inaccurate values.

Comparison of combustion efficiency based on CO/CO2 production was not done due to technical limitations faced at the time. However, since ignition behaviour was mostly looked upon, this was not considered a strict requirement.

The randomness and complexities with wildland fuels makes it difficult to characterize their fire behaviour. The pine needles, like most wildland fuels, are complex and has random orientations. Their individual structure, the way they are oriented inside the sample basket, etc. would result in uneven permeability of the sample. Although in Eq. (2.3) there is a relation of permeability with porosity provided, this is fitted to engineered results, as stated in Santoni *et al.*, (2014). According to this relation, permeability does not depend on the orientation of needles inside a sample of a specific porosity, which would not be true in a realistic scenario where there will be localised density difference inside the sample.

One of the main constraints in studying their ignition behaviour is preparing the sample itself. It took about 1-2 hours to prepare a single pine needle sample and there was a physical limitation in the porosity that could be achieved using 63% sample baskets. If the pine needles were cut

into shorter pieces to accommodate inside the sample basket, they would just fall through the openings. An experiment with wood cribs using thin strips of wood that resembles pine needles (preferably with similar thermophysical properties) may be tested under similar conditions and compared with this test to find out how the ignition behaviour differs. The porosity of the sample should be calculated with the same equation used in this thesis to obtain comparable results.

The impact of external heat flux on heat release rate was analysed on samples of same porosity and it was observed that the heat release rate was independent of the external heat flux between the range 20-40 kW/m^2. However, considerable difference in duration of flaming and peak heat release rate was observed while comparing samples of different porosities under the same external heat flux.

Although the effects of fuel moisture content are one of the most crucial variables, they could not be included in this research. It is strongly believed that further studies should be conducted on this subject.

Developing a heat transfer model for flows through a porous sample driven by heating on the surface would be a strenuous task, considering the mechanisms and processes involved. Even though such a numerical model based on experimental analysis may be able to define the heat transfer in porous wildland fuels to a remarkable extent, the randomness of fuels contributing in a wildfire still maintains the case quite convoluted.

6. Acknowledgement

I would like to thank my supervisor Dr Rory Hadden for his guidance throughout the thesis timeline from deciding the topic to analysing the results. Whenever I had troubles with the experiments or got stuck with thoughts, he had been there to clear my path. He had always been the strongest driving element that motivated me to think different and push my limits.

I would also like to thank Carlos Walker Ravena for the brainstorming sessions and extending his support throughout. He also assisted me with references and always opened my eyes towards things I had missed out. He also got me familiar with the Fire Lab and introduced me to the cone calorimeter. I would also like to my heart-felt gratitude towards Mohamed Beshir and Simon Santamaria for lending a hand over the duration of the experiments and for their valuable advices.

I must thank Grunde Jomaas for his guidance and lectures which turned out to be extremely useful through the process of thesis preparation. He had always been a source of motivation to not be disappointed over setbacks and urged to have fun while working hard.

It is most essential to thank my friends Balsa Jovanovic and James Michael Crum for their assistance throughout, without which completion of this thesis would have been perilous. They had assisted me during most of my experimental sessions and analysis of results.

Mr Michal Krajcovic requires a special thanks for the lab induction and helping me whenever there was a trouble with the cone calorimeter or test methods. I would also like to thank everyone in the John Muir Building who had helped me directly or indirectly throughout my experiments and motivating me throughout the journey.

7. References

A. Nield, D. and Bejan, A. (2006) *Convection in Porous Media*. Third. Springer US.

ASTM E-2058 (2003) 'Users ' Guide for the Fire Propagation Apparatus (FPA)', 44(2). Available at: http://www.fire-testing.com/whitedragon/documents/file/FTT FPA Manual 30-7-03.pdf.

Babrauskas, V. (2003) *Ignition handbook : principles and applications to fire safety engineering, fire investigation, risk management and forensic science*. Issaquah, WA: Fire Science Publishers.

Babrauskas, V. (2016) *The Cone Calorimeter*. Fifth, *SFPE Handbook of Fire Protection Engineering, Fifth Edition*. Fifth. Edited by M. J. Hurley et al. New York, NY: Springer New York. doi: 10.1007/978-1-4939-2565-0.

Bartoli, P. *et al.* (2011) 'Determination of the main parameters influencing forest fuel combustion dynamics', *Fire Safety Journal*. Elsevier, 46(1–2), pp. 27–33. doi: 10.1016/j.firesaf.2010.05.002.

Bartoli, P. (2011) *Feux de forêt : amélioration de la connaissance du couplage combustible-flamme*. UNIVERSITE DE CORSE-PASCAL PAOLI; UNIVERSITY OF EDINBURGH.

Bartoli, P. *et al.* (2015) 'A study on forest fuel combustion dynamics using the Fire Propagation Apparatus', *Combustion*, (July 2015), pp. 2–7.

Bejan, A. and Kraus, A. D. (2003) *Heat Transfer Handbook*. Hoboken, New Jersey: John Wiley & Sons, Inc.

BS ISO 5660-1-2015 (2015) *Reaction-to-fire tests-Heat release, smoke production and mass loss rate-Part 1: Heat release rate (cone calorimeter method) and smoke production rate (dynamic measurement)*. BSI.

C. M. Belcher (2013) *Fire Phenomena and the Earth System: An Interdisciplinary Guide to Fire Science.*

Dakka, S. M., Jackson, G. S. and Torero, J. L. (2002) 'Mechanisms controlling the degradation of poly(methyl methacrylate) prior to piloted ignition', *Proceedings of the Combustion Institute*, 29(1), pp. 281–287. doi: 10.1016/S1540-7489(02)80038-4.

Drysdale, D. (2011) *An Introduction to Fire Dynamics*. Third. Chichester, UK: John Wiley & Sons, Ltd. doi: 10.1002/9781119975465.

Finney, M. A. *et al.* (2015) 'Role of buoyant flame dynamics in wildfire spread', *Proceedings of the National Academy of Sciences*, 112(32), pp. 9833–9838. doi: 10.1073/pnas.1504498112.

Girods, P. *et al.* (2011) 'Comparison of Pyrolysis Behavior Results between the Cone Calorimeter and the Fire Propagation Apparatus Heat Sources', *Fire Safety Science*. Maryland, USA, 10, pp. 889–901. doi: 10.3801/IAFSS.FSS.10-889.

Grishin, A. M. *et al.* (2002) 'Ignition of combustible forest materials by a radiant energy flux', *Combustion, Explosion and Shock Waves*, 38(1), pp. 24–29. doi: 10.1023/A:1014097631884.

Gross, D. (1962) 'Experiments on the burning of cross piles of wood', *Journal of Research of the National Bureau of Standards, Section C: Engineering and Instrumentation*, 66C(2), p. 99. doi: 10.6028/jres.066c.010.

El Houssami, M. *et al.* (2016) 'Experimental and numerical studies characterizing the burning dynamics of wildland fuels', *Combustion and Flame*. Elsevier Inc., 168, pp. 113–126. doi: 10.1016/j.combustflame.2016.04.004.

Howard, E. T. (1971) 'Heat of Combustion of Various Southern Pine Materials', *Wood Science*, 5(3), pp. 194–197. Available at: http://www.srs.fs.usda.gov/pubs/24165.

Howard, E. T. (1973) 'Properties of southern pine needles', *Wood Science*, 5 (4)(April), pp. 281–286. doi: 10.1007/1-4020-4904-8.

Janssens, M. (1991) 'Piloted Ignition of Wood':, *Fire and Materials*, 15(4), pp. 151–167. doi: 10.1002/fam.810150402.

Jervis Calle, F. X. (2012) *Application of fire calorimetry to understand factors affecting flammability of cellulosic material: Pine needles, tree leaves and chipboard*. The University of Edinburgh.

Jervis, F. X. and Rein, G. (2016) 'Experimental study on the burning behaviour of Pinus halepensis needles using small-scale fire calorimetry of live, aged and dead samples', *Fire and Materials*, pp. 385–395. doi: 10.1002/fam.2293.

Karyaparambil, D. D. (2017) *Fire test methods*. Edinburgh.

Lindholm et al., 2009 (2009) 'Cone Calorimeter – a Tool for Measuring Heat', *Åbo Akademi Process*

Chemistry Centre, Finland.

McAllister, S. and Finney, M. (2016) 'Burning Rates of Wood Cribs with Implications for Wildland Fires', *Fire Technology*. Springer US, 52(6), pp. 1755–1777. doi: 10.1007/s10694-015-0543-5.

De Mestre, N. J. *et al.* (1989) 'Uniform Propagation of a Planar Fire front Without Wind', *Combustion Science and Technology*, 65(4–6), pp. 231–244. doi: 10.1080/00102208908924051.

Mindykowski, P. *et al.* (2011) 'Piloted ignition of wildland fuels', *Fire Safety Journal*. Elsevier, 46(1–2), pp. 34–40. doi: 10.1016/j.firesaf.2010.09.003.

National Wildfire Coordinating Group. (1998) 'Wildfire Prevention Strategies', (March). Available at: Wildfire Prevention strategies.pdf.

NIFC (2017) 'Federal Firefighting Costs (Suppression Only) [table]', p. 1987. Available at: https://www.nifc.gov/fireInfo/fireInfo_documents/SuppCosts.pdf.

Quintiere., J. G. (2006) *Fundamentals of Fire Phenomena - Compartment Fires*. Chichester, England : John Wiley.

Ravena, C. W. (2019) *UNDERSTANDING THE HEAT TRANSFER, PYROLYSIS AND IGNITION OF WILD LAND FUELS*. Edinburgh.

Rohsenow, W. M. and Hartnett, J. R. (1998) *HANDBOOK OF HEAT TRANSFER*. Third. New York: MCGRAW-HILL.

Santoni, P. A. *et al.* (2014) 'Bulk and particle properties of pine needle fuel beds – influence on combustion', *International Journal of Wildland Fire*, 23(8), p. 1076. doi: 10.1071/wf13079.

Schemel, C. F. *et al.* (2008) 'A calorimetric study of wildland fuels', *Experimental Thermal and Fluid Science*, 32(7), pp. 1381–1389. doi: 10.1016/j.expthermflusci.2007.11.011.

Schemel, C. F. (2008) 'Transport Effects on Calorimetry of Porous Wildland Fuels', *Philosophy*.

Scott, A. C. (2000) 'The Pre-Quaternary history of fire', 164, pp. 281–329.

Simeoni, A. (2011) 'On the Role of Bulk Properties and Fuel Species on the Burning Dynamics of Pine Forest Litters', *Fire Safety Science*, 10(3), pp. 459–470. doi: http://dx.doi.org/10.3801/IAFSS.FSS.10-1401.

Simeoni, A. *et al.* (2012) 'Flammability studies for wildland and wildland–urban interface fires applied to pine needles and solid polymers', *Fire Safety Journal*. Elsevier, 54, pp. 203–217. doi: 10.1016/j.firesaf.2012.08.005.

Thomas, J. C. *et al.* (2014) 'Flammability study of pine needle beds', *Fire Safety Science*, 11, pp. 1406–1419. doi: 10.3801/IAFSS.FSS.11-1406.

Thomas, J. C. (2017) *Improving the understanding of fundamental mechanisms that influence ignition and burning behavior of porous wildland fuel beds*, *PQDT - UK & Ireland*. The University of Edinburgh. Available at: http://hdl.handle.net/1842/28916.

Thomas, J. C., Hadden, R. M. and Simeoni, A. (2017) 'Experimental investigation of the impact of oxygen flux on the burning dynamics of forest fuel beds', *Fire Safety Journal*. Elsevier Ltd, 91(May), pp. 855–863. doi: 10.1016/j.firesaf.2017.03.086.

Tihay, V. *et al.* (2009) 'Experimental study of laminar flames obtained by the homogenization of three forest fuels', *International Journal of Thermal Sciences*. Elsevier Masson SAS, 48(3), pp. 488–501. doi: 10.1016/j.ijthermalsci.2008.03.018.

Torero, J. (2016) *Flaming Ignition of Solid Fuels*. Fifth, *SFPE Handbook of Fire Protection Engineering, Fifth Edition*. Fifth. Edited by M. J. Hurley et al. New York, NY: Springer New York. doi: 10.1007/978-1-4939-2565-0.

U.S. National Park Service (2019) *Wildfire Causes and Evaluations (U.S. National Park Service)*. Available at: https://www.nps.gov/articles/wildfire-causes-and-evaluation.htm (Accessed: 17 March 2019).

Vaz, G. C., André, J. C. S. and Viegas, D. X. (2004) 'Estimation of the radiation extinction coefficient of natural fuel beds', *International Journal of Wildland Fire*, 13(1), pp. 65–71. doi: 10.1071/WF03009.

Wickström, U. (2016) *Methods for Predicting Temperatures in Fire-Exposed Structures*. Fifth, *SFPE Handbook of Fire Protection Engineering, Fifth Edition. Fifth*. Fifth. Edited by M. J. Hurley et al. New York, NY: Springer New York. doi: 10.1007/978-1-4939-2565-0.